Cell Reports

Resource

# Spatial and temporal proteomics reveals the distinct distributions and dynamics of O-GlcNAcylated proteins

## Graphical abstract

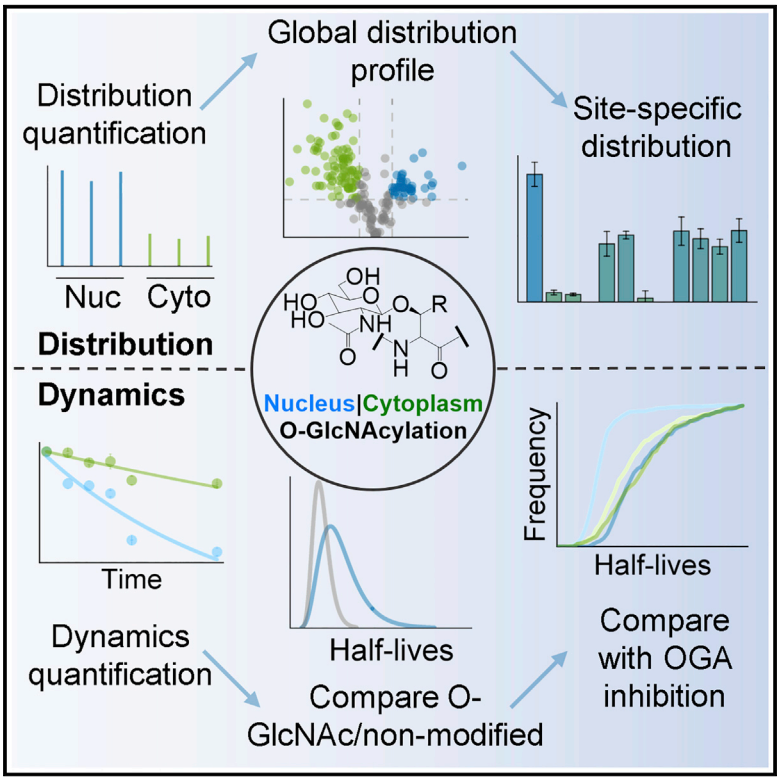


## Highlights

- O-GlcNAcylated proteins with different functions have distinct distributions
- The distributions of O-GlcNAcylated proteins vary site specifically
- Cytoplasmic O-GlcNAcylated proteins are generally more stable than nuclear proteins
- Glycoproteins are more stabilized in the nucleus under the OGA inhibition

## Authors

Senhan Xu, Ming Tong, Suttipong Suttapitugsakul, Ronghu Wu

## Correspondence

ronghu.wu@chemistry.gatech.edu

## In brief

Xu et al. systematically and site specifically study the distribution and dynamics of O-GlcNAcylated proteins in the nucleus and the cytoplasm. O-GlcNAcylated proteins with different functions have distinct distribution patterns. The half-lives of glycoproteins in the two cellular compartments are markedly different, with the much longer median half-life in the cytoplasm.

Xu et al., 2022, Cell Reports *39*, 110946
June 14, 2022
https://doi.org/10.1016/j.celrep.2022.110946

CellPress

Cell Reports

CellPress
OPEN ACCESS

Resource

# Spatial and temporal proteomics reveals the distinct distributions and dynamics of O-GlcNAcylated proteins

Senhan Xu,[1] Ming Tong,[1] Suttipong Suttapitugsakul,[1] and Ronghu Wu[1,2,*]
[1]School of Chemistry and Biochemistry and the Petit Institute for Bioengineering and Bioscience, Georgia Institute of Technology, Atlanta, GA 30332, USA
[2]Lead contact
*Correspondence: ronghu.wu@chemistry.gatech.edu
https://doi.org/10.1016/j.celrep.2022.110946

## SUMMARY

Protein O-GlcNAcylation plays critical roles in many cellular events, and its dysregulation is related to multiple diseases. Integrating bioorthogonal chemistry and multiplexed proteomics, we systematically and site specifically study the distributions and dynamics of protein O-GlcNAcylation in the nucleus and the cytoplasm of human cells. The results demonstrate that O-GlcNAcylated proteins with different functions have distinct distribution patterns. The distributions vary site specifically, indicating that different glycoforms of the same protein may have different distributions. Moreover, we comprehensively analyze the dynamics of O-GlcNAcylated and non-modified proteins in these two compartments, respectively, and the half-lives of glycoproteins in different compartments are markedly different, with the median half-life in the cytoplasm being much longer. In addition, glycoproteins in the nucleus are more dramatically stabilized than those in the cytoplasm under the O-GlcNAcase inhibition. The comprehensive spatial and temporal analyses of protein O-GlcNAcylation provide valuable information and advance our understanding of this important modification.

## INTRODUCTION

Protein O-GlcNAcylation refers to the enzymatic modification of the serine and threonine residues with N-acetylglucosamine (GlcNAc). Unlike other types of glycosylation normally on proteins in the classical secretory pathway, O-GlcNAcylation mainly occurs on proteins in the nucleus and the cytoplasm (Alfaro et al., 2012; Hart et al., 2007). Since its discovery, O-GlcNAcylation has attracted great attention due to its importance in biological systems, including the regulation of gene expression and signal transduction (Hart et al., 2011; Torres and Hart, 1984; van der Laarse et al., 2018). Aberrant protein O-GlcNAcylation is directly related to multiple human diseases, such as diabetes and cancer (Chen et al., 2021; de Queiroz et al., 2016; Hart et al., 2011).

The dynamic nature of protein O-GlcNAcylation is regulated by two enzymes: O-GlcNAc transferase (OGT) and O-GlcNAcase (OGA), which catalyze the addition or removal of O-GlcNAc to or from protein substrates, respectively (Joiner et al., 2019; Li et al., 2017). It was reported that O-GlcNAcylation can regulate protein degradation (Levine et al., 2019; Yang et al., 2006). For example, O-GlcNAcylation can protect many proteins from proteasomal degradation, such as p53, C-myc, DOT1L, and Nrf1, through the crosstalk with phosphorylation and ubiquitination (de Queiroz et al., 2016; Han et al., 2017; Luanpitpong et al., 2020; Song et al., 2021), or by recruiting deubiquitinases (Baldini et al., 2016; Ruan et al., 2012). It can also prevent α-synuclein from aggregation and proteolytic cleavage by calpain (Levine et al., 2017; Marotta et al., 2015). In serum, O-GlcNAcylation was able to stabilize the synthetic peptides, even with the O-GlcNAcylation sites being 10–15 amino acids away from the cleavage site (Levine et al., 2019). Furthermore, O-GlcNAcylation can modify proteins in the 26S proteosome to inhibit the proteolysis (Zhang et al., 2003).

Besides protein dynamics, O-GlcNAcylation can regulate protein translocation, in which the subcellular localization of O-GlcNAcylated proteins is critical for their functions. For instance, O-GlcNAcylation can induce the translocation of the transcription factor neurogenic differentiation factor 1 (NeuroD1) to the nucleus under high glucose conditions to regulate the gene expression (Andrali et al., 2007). O-GlcNAcylation was also reported to activate the transcription factor nuclear factor κB (NF-κB) and promote its translocation to the nucleus (Yang et al., 2008). Moreover, O-GlcNAcylation at certain sequence motifs can help the binding of cargo proteins to importin α to facilitate their nuclear transport (Tan et al., 2021). Considering the importance of O-GlcNAcylation in cells, global and site-specific study of the spatial distribution and the dynamics of O-GlcNAcylation proteins will result in an in-depth understanding of this important modification.

In this work, we systematically and site specifically quantified the distribution and dynamics of O-GlcNAcylated proteins in the nucleus and the cytoplasm by integrating bioorthogonal chemistry and multiplexed proteomics. The results demonstrated that O-GlcNAcylated proteins with different functions have distinct distribution patterns. Benefitting from the site-specific analysis,

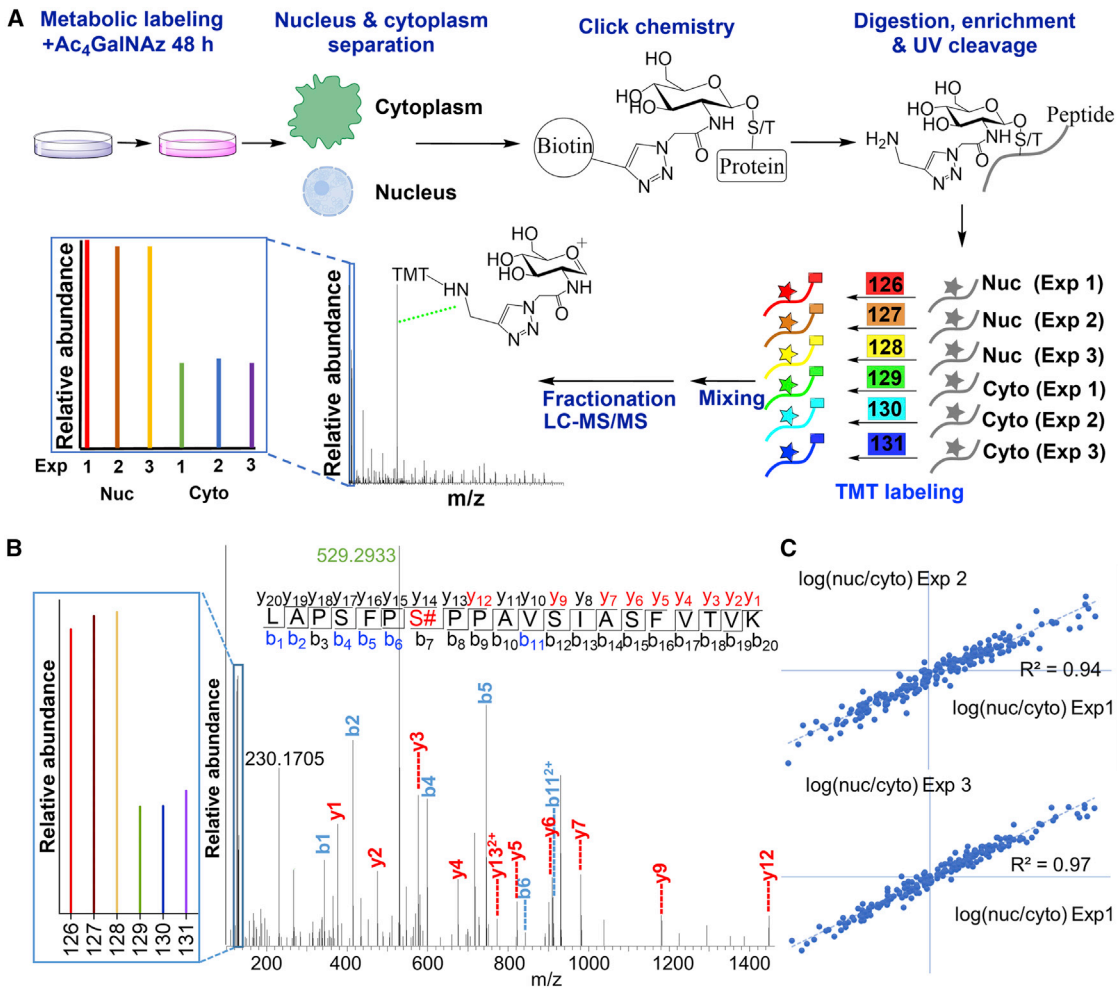


**Figure 1. Quantification of the distributions of O-GlcNAcylated proteins in the nucleus and the cytoplasm**

(A) Experimental procedure for analyzing the distributions of O-GlcNAcylated proteins in the nucleus and the cytoplasm.

(B) Example MS/MS spectrum of an O-GlcNAcylated peptide identified. The inset shows the reporter ion intensities. The peak with *m/z* = 529.2932 is from the protonated modified GlcNAc moiety.

(C) Reproducibility of the results from the biological triplicate experiments. Each data point represents the $\log_2$(ratio) for the distribution of a unique glycopeptide quantified in 2 replicates.

See also Figure S1.

unique O-GlcNAcylation sites were found to differentially regulate the distribution of the same protein. The half-lives of O-GlcNAcylated proteins in the two compartments were quantified along with those of non-modified proteins. The results revealed that the degradation of O-GlcNAcylated proteins in different compartments were markedly different, with the median half-life of O-GlcNAcylated proteins in the cytoplasm being much longer than that in the nucleus. The degradation rates of O-GlcNAcylated proteins are mostly slower than the non-modified counterparts in both compartments. Furthermore, to understand the effect of OGA on the dynamics of O-GlcNAcylated proteins, the half-lives of O-GlcNAcylated proteins in the two compartments were quantified under the OGA inhibition. Glycoproteins in the nucleus were more dramatically stabilized than those in the cytoplasm under the inhibition, indicating the more active removal of the glycan by OGA in the nucleus. Spatial and temporal investigation of protein O-GlcNAcylation in human cells provides valuable information about this important glycosylation.

## RESULTS

### Quantification of the distributions of O-GlcNAcylated proteins in the nucleus and the cytoplasm

We designed a method integrating metabolic labeling, bioorthogonal chemistry, and multiplexed proteomics to systematically quantify the distribution of O-GlcNAcylated proteins in the nucleus and the cytoplasm (Figure 1A). The integration of metabolic labeling and bioorthogonal chemistry is very powerful to study protein glycosylation (Agatemor et al., 2019; Mahal et al., 1997; Qin et al., 2017; Suttapitugsakul et al., 2019, 2021a, 2021b; Vocadlo et al., 2003; Woo et al., 2015). Glycoproteins were metabolically labeled with *N*-azidoacetylgalactosamine-tetraacetylated

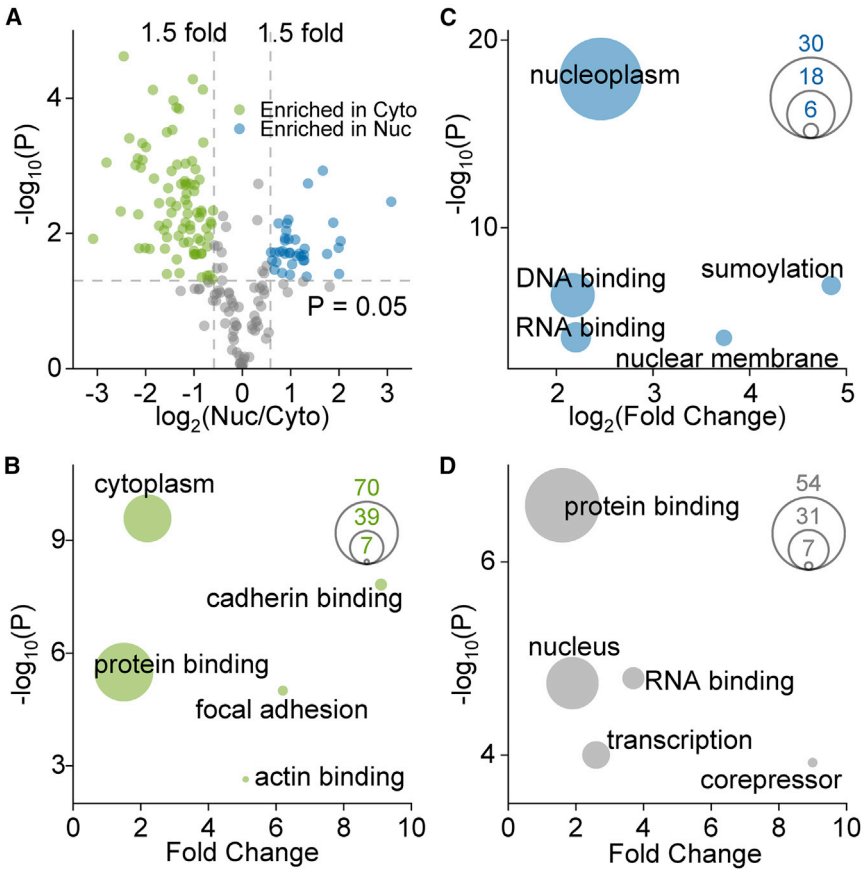


**Figure 2. Analysis of the distributions of O-GlcNAcylated proteins in the nucleus and the cytoplasm**

(A) Distributions of O-GlcNAcylated proteins enriched in the cytoplasm, the nucleus, or neither compartment (n = 3 biological replicates). p values were determined using the one sample t test, null hypothesis: mean = 0, two-tailed.

(B–D) The proteins in each category were clustered based on cellular compartment, biological process, and molecular function. The results for the cytoplasm-enriched proteins are in (B), the nucleus-enriched proteins in (C), and those not enriched in either compartment are in (D). The size of the circles is proportional to the number of proteins in each category. p values were determined using Fisher's exact test, 1-tailed in (B)–(D).

See also Figure S2 and Table S1.

($Ac_4GalNAz$) (Boyce et al., 2011; Xiao et al., 2016), and labeled glycoproteins with the small azide group allowed for their selective enrichment through bioorthogonal chemistry (Hong et al., 2009). Subsequently, cells were harvested and lysed with a buffer containing a low concentration of a mild detergent that preserved the nuclear envelope. The nuclear and cytoplasmic fractions were separated by centrifugation, as reported previously (Martynova et al., 2021; Nabbi and Riabowol, 2015; Suzuki et al., 2010). To evaluate the separation of nuclear and cytoplasmic proteins, trypan blue staining and western blot experiments were performed. The results demonstrated the successful separation of proteins in the nucleus and the cytoplasm (Figure S1).

The azide-labeled glycoproteins were then tagged with the alkyne photocleavable (PC)-biotin reagent. After tryptic digestion, glycopeptides with the biotin tag were enriched and released from the resins under UV radiation. The cleavage also generated an amine group on the glycan that facilitates the protonation of glycopeptides for mass spectrometry (MS) analysis. To quantify the relative amount of each O-GlcNAcylated protein in the nucleus and the cytoplasm, multiplexed proteomics was used. In the biological triplicate experiments, six samples (three nuclear samples and three cytoplasmic samples) were labeled with six channels of the tandem mass tag (TMT) reagents. After the labeling, six samples were mixed, purified, and fractionated before liquid chromatography (LC)-MS analysis.

One example glycopeptide identified, LAPSFPS#PPAVSIASFVTVK (# denotes the glycosylation site), from pogo transposable element with ZNF domain (POGZ) is in Figure 1B. The glycopeptide is confidently identified with an XCorr of 3.63, a mass accuracy of −1.69 ppm, and a ModScore of 22.49. The presence of a modified GlcNAc on the peptide is further supported by the fragment with $m/z$ = 529.2932, which matches very well with the mass of the modified GlcNAc (protonated). To obtain the distributions of O-GlcNAcylated proteins, the ratios were calculated from the TMT reporter ion intensities for glycopeptides in the nucleus and the cytoplasm in each experiment. The reproducibility across these biological replicates was evaluated, and the correlations among the triplicates were reasonably high (Figure 1C).

## Analysis of O-GlcNAcylated proteins enriched in the nucleus and the cytoplasm

To determine whether an O-GlcNAcylated protein was enriched in the nucleus or the cytoplasm, glycoproteins with the average protein ratio from the triplicate experiments greater than 1.5-fold are considered to be enriched in the nucleus, while those with the average ratio lower than 0.67-fold are enriched in the cytoplasm with $p < 0.05$ (the one-sample t test, null hypothesis: mean = 0, two-tailed). Among 195 O-GlcNAcylated proteins quantified here, 36 were found to be enriched in the nucleus, 85 were in the cytoplasm, and 74 were not enriched in either compartment (Figure 2A; Table S1). The quantified glycoproteins in each group were clustered based on their Gene Ontology (GO) terms (Figures 2B–2D). GO terms including nucleoplasm, nuclear membrane, DNA binding, RNA binding, and protein SUMOylation are significantly overrepresented among the nucleus-enriched glycoproteins. On the contrary, among the cytoplasm-enriched glycoproteins, the terms including "cytoplasm," "protein binding," "focal adhesion," "actin binding," and "cadherin binding" are overrepresented. Glycoproteins that are not specifically enriched

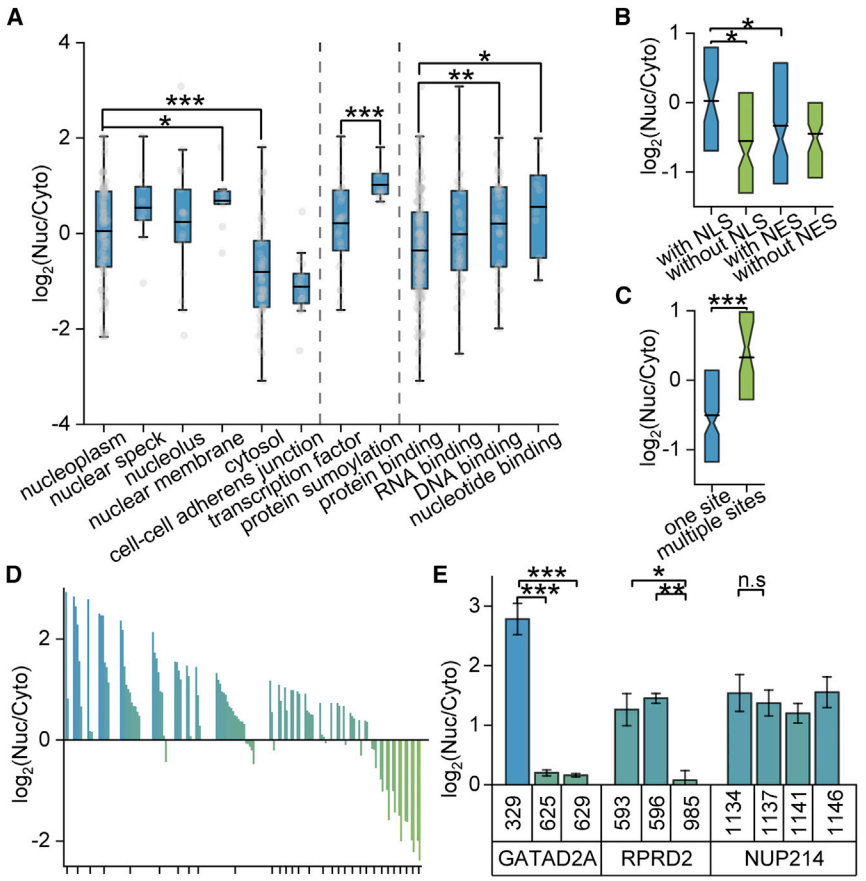


**Figure 3. Regulation of the protein distribution by O-GlcNAcylation**

(A) Comparison of the distribution of O-GlcNAcylated proteins related to different clusters based on cellular compartment, biological process, and molecular function. The results are displayed as boxplots, with each component separated by the dashed lines. Center line: mean value. Box: 25th/75th percentiles. Whiskers: upper/lower inner fences. The gray dots behind each box: the $\log_2$(ratio) of each protein in this category.

(B) Comparison of the distribution of O-GlcNAcylated proteins with or without NLS and NES.

(C) Distribution of O-GlcNAcylated proteins with single or multiple O-GlcNAcylation sites on each protein. Box: 25th/75th percentiles. Center line: mean value.

(D) Graphic view of the $\log_2$(ratio) measured for each quantified O-GlcNAcylation site. Each tick on the horizontal axis represents an O-GlcNAcylated protein.

(E) Example proteins from (D) with quantified O-GlcNAcylation sites (data are represented as means ± SEMs, n = 3 biological replicates). The differences are assessed by the 2-sample t test, 2-tailed, and the significance levels are labeled *p < 0.05, **p < 0.01, and ***p < 0.001.

See also Tables S2 and S3.

in either compartment are involved in RNA binding, transcription, and transcription repressor, indicating that many glycoproteins participating in transcription and mRNA processing are more equally distributed in both the nucleus and the cytoplasm. These observations reveal the different distributions of O-GlcNAcylated proteins with different functions in the nucleus or the cytoplasm.

To better understand the distributions of O-GlcNAcylated proteins, we performed further analyses. Glycoproteins with the "nucleoplasm" annotation have a significantly higher average ratio than those annotated with "cytosol" (Figure 3A). Alternatively, glycoproteins related to "nuclear membrane" have a significantly greater distribution in the nucleus than those related to "nucleoplasm." This may be because the glycoproteins in the nuclear membrane are mostly structural components of the nuclear pore complex (NPC) (Ruba and Yang, 2016), yet some proteins in the nucleoplasm can more easily shuttle between the nucleus and the cytoplasm (Gama-Carvalho and Carmo-Fonseca, 2001). The O-GlcNAcylated transcription factors identified have a median ratio close to 1. Proteins related to "DNA binding" and "nucleotide binding" have much greater distributions in the nucleus than those annotated with "protein binding," consistent with our finding that many glycoproteins enriched in the nucleus are involved in nucleic acid binding, while those enriched in the cytoplasm are related more to protein binding.

## Unraveling the mechanisms of the regulation of protein distribution by O-GlcNAcylation

As O-GlcNAcylated proteins with various functions could have different distributions, it is interesting to determine how O-GlcNAcylated proteins are regulated to be transported in and out of the nucleus. Many proteins can shuttle between the nucleus and the cytoplasm through the NPC (Lamond and Earnshaw, 1998). For proteins to be transported into the nucleus, a certain exposed amino acid sequence called nuclear transport signal (NLS) of a protein could interact with the protein importin $\alpha$, which is a part of the complex responsible for protein transportation into the nucleus (Lange et al., 2007). Conversely, nuclear export signal (NES) serves as a tag for proteins to be translocated back to the cytoplasm (Fu et al., 2018). We compared the distribution ratios of glycoproteins with and without NLS or NES (Figure 3B), and the results demonstrate that glycoproteins with NLS are more enriched in the nucleus compared with those without NLS. On the contrary, no significant difference was observed when the distributions of glycoproteins with and without NES were compared.

Previous studies showed that other factors may play critical roles in the regulation of nuclear protein transportation, including protein post-translational modifications (PTMs) (Poon and Jans, 2005). For example, phosphorylation in the

vicinity of NLS could diminish the sequence positive charge and reduce its binding to importin (Harreman et al., 2004). O-GlcNAcylation was found to mediate nuclear translocation of NF-κB by interrupting its interaction with IκBα (nuclear factor of kappa light polypeptide gene enhancer in B cells inhibitor, alpha) (Yang et al., 2008). Another mechanism for O-GlcNAcylation to regulate the translocation of nuclear proteins is through its crosstalk with phosphorylation. For example, phosphorylation and O-GlcNAcylation regulate the nuclear or cytoplasmic localization of tau (Lefebvre et al., 2003). Given the potential effect of O-GlcNAcylation on protein translocation between the nucleus and the cytoplasm, we investigated the correlation between the number of O-GlcNAcylation sites and the protein distribution. Glycoproteins are separated into two groups based on the number of O-GlcNAcylation sites on each protein (i.e., single or multiple). Proteins identified with multiple sites have a significantly higher distribution in the nucleus than those with one site (Figure 3C), which suggests that more O-GlcNAcylation events are correlated with the higher distribution of glycoproteins in the nucleus.

## Site-specific regulation of the protein distribution by O-GlcNAcylation

As O-GlcNAc on a certain site of proteins can affect their structures and interactions, different O-GlcNAcylation sites on a glycoprotein may distinctively regulate the glycoprotein distribution. Here, the results for the distribution based on unique glycopeptides and well-localized sites were calculated and plotted (Figures S2A and S2B), and the distributions of O-GlcNAcylated proteins based on well-localized sites are included (Table S2). All of the glycoproteins with more than one well-localized site were extracted, and a graphic view of the ratios measured for all of the glycosylation sites in each protein is displayed in Figure 3D.

Within each detected protein, we performed the two-sample t test for the ratios between every two different glycosylation sites measured in the biological triplicate experiments. Among 31 proteins tested, 17 have at least 2 glycosylation sites with significantly different ratios (Table S3), indicating that the same protein with different sites could have different distributions. For example, transcriptional repressor p66-alpha (GATAD2A) has the distribution ratio of T329 close to 8, while S625 and S629 have the ratio of approximately 1, revealing that only the glycoform with the T329 site is highly enriched in the nucleus (Figure 3E). For another protein, the regulation of nuclear pre-mRNA domain-containing protein 2 (RPRD2), the glycosylation sites S593 and S596 have the ratios of approximately 2, while T985 has a ratio near 1, demonstrating that the glycoforms of the protein with the S593 or S596 site have a higher nuclear distribution than the same protein with the glycosylated T985. On the contrary, NUP214 shows no significant difference in the distributions among all of the quantified sites. NUP214 is a subunit of the NPC, and the glycosylation of NUP214 is important for the functions of the complex (Zhu et al., 2016). However, it may have little effect on the protein distribution. These results provide valuable site-specific information for the distributions of O-GlcNAcylated proteins.

## Spatial-resolved investigation of the dynamics of O-GlcNAcylated proteins in the nucleus and the cytoplasm

Due to the heterogeneity of the microenvironment in cells, the same glycoprotein may have distinct dynamics in different cellular compartments, but the spatial and systematic study of the dynamics of O-GlcNAcylated proteins remains to be explored. In addition, O-GlcNAcylation could protect a wide range of proteins from degradation, but the effect on the proteome scale is rarely explored. Here, we simultaneously quantified the dynamics of proteins with and without O-GlcNAcylation in the nucleus and the cytoplasm by a pulse-chase method (Figure 4A). Cells grew in the normal culture medium with $Ac_4$GalNAz. During the chase period, $Ac_4$GalNAz was substituted by $Ac_4$GalNAc, while light amino acids (K0 and R0) were replaced with heavy amino acids (K8 and R6). Then, cells from different time points were split into nuclear and cytoplasmic fractions, and each fraction was further separated for O-GlcNAcylated protein and whole proteome analyses. The peptide samples were labeled with TMT before mixing, and the degradation profiles of O-GlcNAcylated/non-modified proteins over time (0, 3, 6, 9, 12, and 24 h) were recorded.

The site-specific and spatial quantification of glycoproteins reveals their independent degradation rates in both the nucleus and the cytoplasm. For some sites of the same proteins, the degradation rates are very similar in the two compartments. For example, glycosylation at S395 on TAB1 has very similar half-lives in the nucleus and the cytoplasm (Figure 4B), and the same is true for S403 on GMEB2 (Figure S3A). In contrast, some sites have dramatically different degradation rates in the two compartments. For instance, S297 from POGZ is very stable in the cytoplasm, while the same site of the same protein has a much higher degradation rate in the nucleus (Figure 4C). Similarly, S410 on LDB1 (Figure 4D) and S1154 on NFRKB (Figure 4E) have much higher degradation rates in the nucleus than in the cytoplasm.

For many O-GlcNAcylated proteins, all of the glycosylation sites from the same protein have longer half-lives in the cytoplasm than in the nucleus, such as different sites on ZFR and SMG7 (Figures 4F and S3B). On the contrary, for ADRM1, the two sites have longer half-lives in the nucleus than in the cytoplasm (Figure 4G). For some proteins with multiple sites, their degradation rates may be similar among these sites in both compartments. For instance, three sites on ATF7IP have very similar half-lives (Figure 4H).

The half-lives of O-GlcNAcylated proteins in the nucleus and the cytoplasm were quantified in the duplicate experiments. The overlap between the duplicate experiments is reasonably high (Figure S4A). In total, 244 O-GlcNAcylated proteins were identified from the nucleus and 212 from the cytoplasm (Figure 5A; Tables S4 and S5). Among these proteins, 139 glycoproteins were identified only in the nucleus, while 107 were identified exclusively in the cytoplasm. Moreover, 105 glycoproteins were identified in both compartments. The half-life distributions of O-GlcNAcylated proteins in the nucleus and the cytoplasm from the duplicate experiments are very similar

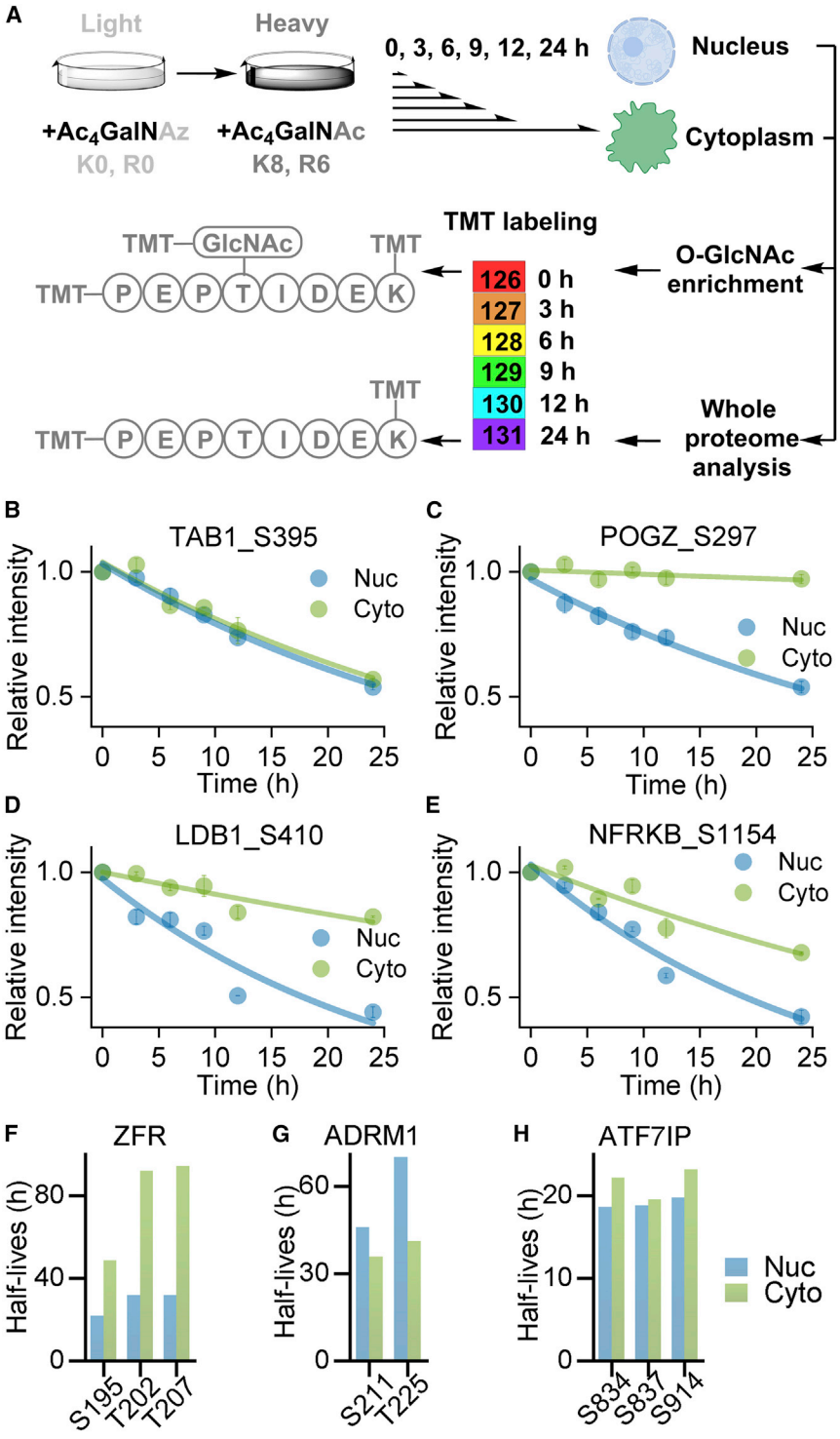


**Figure 4. Systematic quantification of the dynamics of the glycosylated and non-modified forms of proteins in the nucleus and the cytoplasm**

(A) Experimental design to systematically quantify the dynamics of the glycosylated and non-modified forms of proteins in the 2 cellular compartments.

(B–E) Examples of the glycopeptide degradation. Data are represented as means ± SEMs (n = 2 biological replicates).

(F–H) Examples of site-specific quantification of the half-lives of O-GlcNAcylated proteins in the nucleus and the cytoplasm.

See also Figure S3.

(Figures 5B and 5C). Overall, the current results demonstrate that O-GlcNAcylated proteins in the cytoplasm are generally more stable than the nuclear proteins, but the differences can vary for each individual glycoprotein and even for each glycosylation site.

The glycoproteins quantified in each compartment were subsequently ranked based on their half-lives and separated into three groups with an equal number of proteins (short, medium, and long). Those proteins associated with repressor, transcription, viral process, DNA binding, and sequence features including polyalanine, proline, serine, and threonine-rich are enriched among the short-lived glycoproteins in the cytoplasm. Conversely, proteins related to RNA binding, zinc ion binding, and LIM domain, and with sequence features like asparagine-rich, are overrepresented in the long-lived cytoplasmic glycoproteins (Figure 5D). Similar analyses were performed for the nuclear O-GlcNAcylated proteins, and it was found that the chromatin regulators and the proteins with glutamine and threonine-rich sequences are highly enriched for the short-lived proteins. In contrast, glycoproteins related to nucleotide binding, mRNA splicing, nuclear envelope, and with poly-alanine sequence are overrepresented among the long-lived glycoproteins in the nucleus (Figure 5E).

The half-lives of the same glycoproteins quantified in both compartments were plotted in Figure S4B. To investigate whether the half-life differences of glycoproteins in different compartments are correlated with their nuclear-cytoplasmic distributions, we used the data for the glycoprotein distributions quantified earlier (Table S1). The glycoproteins were separated into three groups based on the difference of the half-lives in the nucleus and the cytoplasm for each protein. We found that the group with longer nuclear half-lives had a significantly higher cytoplasmic distribution (Figure 5F).

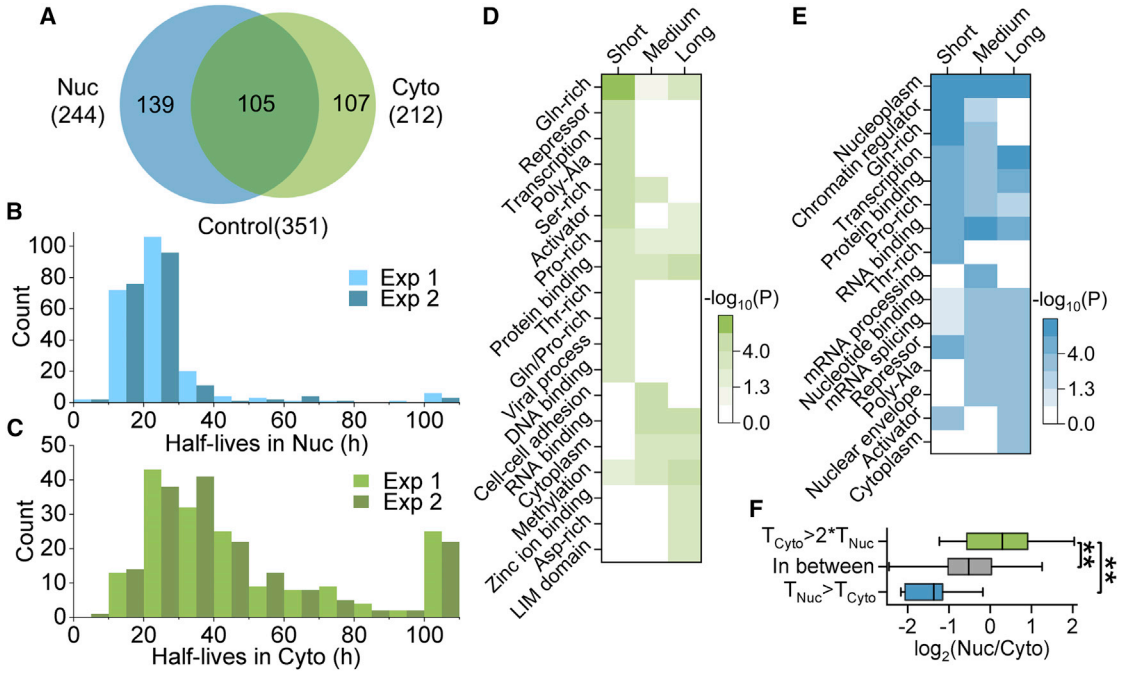


**Figure 5. Evaluation of the half-lives of O-GlcNAcylated proteins in the nucleus and the cytoplasm**

(A) Overlap of O-GlcNAcylated proteins quantified in the nucleus and the cytoplasm from the duplicate experiments.

(B and C) Half-life distributions of O-GlcNAcylated proteins in the nucleus (B) and the cytoplasm (C) from the duplicate experiments.

(D and E) Analysis of O-GlcNAcylated proteins with different half-lives in the cytoplasm (D) and the nucleus (E) based on cellular compartment, biological process, molecular function, and sequence feature.

(F) Comparison of the half-life differences with the distributions of O-GlcNAcylated proteins. The glycoproteins are separated into 3 groups based on the comparison of their half-lives in the nucleus and the cytoplasm of each protein. Glycoproteins with longer half-lives in the nucleus are included in the group "$T_{nuc} > T_{cyto}$." Those with cytoplasmic half-lives >2 times longer than the nuclear half-lives are included in "$T_{cyto} > 2*T_{nuc}$." The rest is in the group "in between." Center line: mean value. Box: 25th/75th percentiles. Whiskers: upper/lower inner fences. The differences between the groups are calculated by the 2-sample t test, 2-tailed, and the significance levels are labeled *$p < 0.05$, **$p < 0.01$, and ***$p < 0.001$.

See also Figure S4 and Tables S4 and S5.

## Systematic study of the effect of O-GlcNAcylation on protein degradation

It was reported that O-GlcNAcylation can prevent some proteins from degrading (Ruan et al., 2013), but a systematic study of this effect at the proteome scale remains to be studied. We simultaneously recorded the degradation profiles of the O-GlcNAcylated and non-modified forms of proteins in the nucleus and the cytoplasm, respectively (Figure 4A). In each compartment, the proteins quantified with both the O-GlcNAcylated and non-modified forms were used for comparison to study the effect of O-GlcNAcylation on protein dynamics. With this approach, 217 and 174 proteins in the nucleus and the cytoplasm were quantified for the modified and non-modified forms (Table S6). The median half-lives of O-GlcNAcylated proteins were dramatically longer than the non-modified forms in the two compartments. In the cytoplasm, the median half-life of the non-modified forms is 18.4 h, while that of the glycosylated forms is >2 times longer (38.8 h). The same trend was found in the nucleus (i.e., 15.0 versus 22.5 h [non-modified versus glycosylated]), but the increased magnitude is smaller (Figures 6A and 6B). The current results demonstrate that the protective effect is stronger for proteins in the cytoplasm than in the nucleus.

Next, we investigated the effect of O-GlcNAcylation on the degradation of proteins in different protein complexes. The extent of O-GlcNAcylation altering protein half-lives was represented by the $\log_2$ ratio of the half-life of an O-GlcNAcylated protein divided by that of the corresponding non-modified protein. Proteins in the NPC are heavily O-GlcNAcylated, and it was reported that the knockdown of OGT led to faster turnover of the NPC proteins due to increased ubiquitination and proteasomal degradation (Mizuguchi-Hata et al., 2013; Zhu et al., 2016). We found that all quantified O-GlcNAcylated proteins in the NPC have longer half-lives than their non-modified forms (Figure 6C), including both the peripheral nucleoporins (NUPs) (e.g., NUP153, NUP214) and the scaffold NUPs (NUP93), which is in accordance with the previous report (Zhu et al., 2016).

O-GlcNAcylation was identified on many splicing factors (Mckay and Johnson, 2010) and can control detained intron splicing (Tan et al., 2020). Here, we found that O-GlcNAcylation also stabilized the proteins in the spliceosome (Figure 6C). The majority of O-GlcNAcylated proteins quantified in the nucleolus have longer half-lives than the corresponding non-modified ones, which is consistent with previous reports about some nucleolar proteins being stabilized by O-GlcNAcylation (Chen et al., 2021). O-GlcNAcylation extensively modifies histone

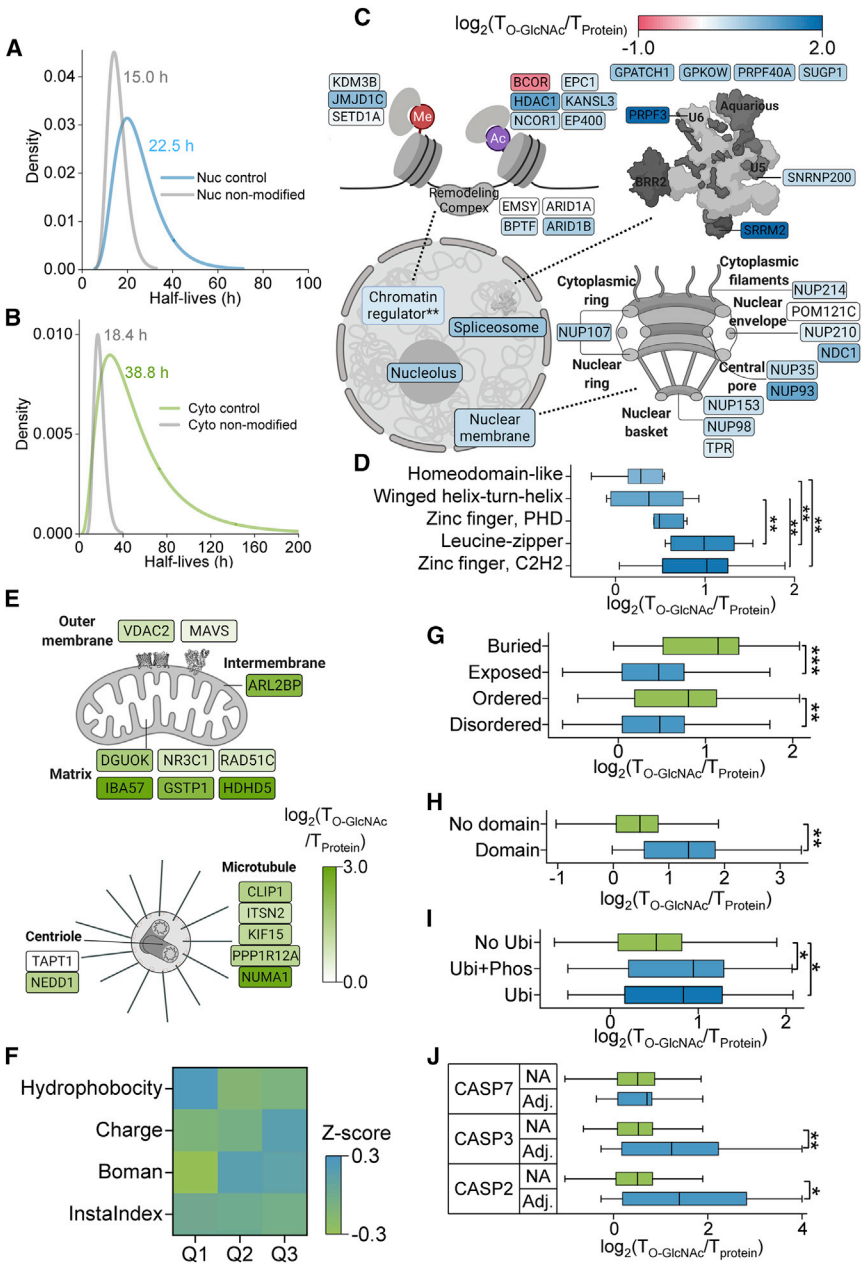


**Figure 6. Effect of O-GlcNAcylation on protein dynamics**

(A and B) Half-life distribution of O-GlcNAcylated proteins and the corresponding non-modified form in the nucleus (A) and the cytoplasm (B). The area under the curve (AUC) represents the number percentage of the proteins with the half-lives in the range.

(C) Effect of O-GlcNAcylation on the dynamics of glycoproteins quantified in different protein complexes in the nucleus.

(D) Effect of O-GlcNAcylation on the dynamics of proteins with different chromatin-binding domains.

(E) Effect of O-GlcNAcylation on protein dynamics in the mitochondrion and the centrosome in the cytoplasm.

(F) Heatmap of *Z* scores transformed from the average of the protein property-related values. Hydrophobicity: GRAVY hydrophobicity index; charge: the net charge of a protein; Boman: potential protein interaction index based on protein sequences (the higher the value, the higher the binding potential); InstaIndex: prediction of protein stability. The values of each protein property were compared for proteins in Q1, Q2, and Q3 and examined by the 2-sample t test.

(G) Evaluation of the correlation between the effect of O-GlcNAcylation on protein dynamics with the protein secondary structures.

(H–J) Comparison of the effect of the O-GlcNAcylation on protein dynamics with whether the glycosylation sites are adjacent to protein domains (H), near the ubiquitination and phosphorylation sites (I), and near the caspase cleavage sites (J). The boxplots followed the same settings. Center line: mean value. Box: 25th/75th percentiles. Whiskers: upper/lower inner fences. The differences between the groups were calculated by the 2-sample t test, 2-tailed, and the significance levels are labeled *p < 0.05, **p < 0.01, and ***p < 0.001.

See also Figure S5 and Table S6.

"writers" and "erasers" to modulate their activities, and one critical means is by mediating the protein stability. For example, histone-lysine *N*-methyltransferase EZH2 (EZH2) (Lo et al., 2018) and lysine *N*-methyltransferase 2E (MLL5) (Ding et al., 2015) were stabilized by O-GlcNAcylation to facilitate their activities. Similarly, we also found many chromatin regulators stabilized by glycosylation (Figure 6C). Nevertheless, some glycoproteins have shorter half-lives compared with the corresponding non-modified form. BCL-6 corepressor (BCOR) was found to be destabilized by O-GlcNAcylation, which is not surprising, as some proteins destabilized by O-GlcNAcylation were already known (Cheng et al., 2016; Srikanth et al., 2010). The average half-life change of glycoproteins as chromatin regulators is significantly less than those of the glycoproteins in other nuclear complexes (Figure 6C), which may be due to glycoproteins related to the regulation of transcription being more dynamic. The $\log_2$ ratios of the glycoproteins containing different domains for the transcription regulation were compared (Figure 6D). The average $\log_2$ ratios for the proteins with C2H2 zinc finger and leucine zipper are significantly higher than those with winged helix-turn-helix and homeodomain-like domains. Our results demonstrate that O-GlcNAcylation has diverse effects on regulating the dynamics of proteins involved in transcription.

Cytoplasmic O-GlcNAcylated proteins are vital in cell homeostasis partly by modulating the functions of the mitochondrion (Zhao et al., 2016) and centrosome (Yuan et al., 2021). It was found that O-GlcNAcylation extensively stabilized proteins in these two organelles (Figure 6E). O-GlcNAcylation was reported to regulate mitochondrial response to oxidative stress through

protecting the proteins from degradation (Ngoh et al., 2011; Zachara et al., 2004). Hyper-O-GlcNAcylation on the centrosomal proteins can interfere with centrosome separation and disrupt the cell cycle (Liu et al., 2020). Here, we found that several O-GlcNAcylated proteins in the centrosome had a longer half-life than its corresponding non-modified form (Figure 6E).

### Effect of O-GlcNAcylation on protein dynamics is related to local structures and the interactions with degrons

To investigate the factors contributing to the effect of O-GlcNAcylation on protein dynamics, we studied the correlation between the half-life differences and protein properties, local structures, and potential crosstalk with other modifications. The nuclear O-GlcNAcylated proteins were ranked based on the half-life ratio between the glycosylated and non-modified forms of each protein. We separated the quantified glycoproteins into three groups with equal numbers. Q1 contains glycoproteins with the lowest $\log_2$ ratio (glycosylated forms with half-lives shorter than or close to the corresponding non-modified ones), while Q3 has the highest ratio. The values for some protein property indices were normalized and compared between the groups (Figure 6F). The glycoproteins with the lowest $\log_2$ ratios (Q1) were significantly more hydrophobic, were more negatively charged, and had fewer protein interactions compared with those having the highest $\log_2$ ratios (Q3) ($p < 0.05$). O-GlcNAc can mediate protein interactions with other molecules (Tarbet et al., 2018). As longer half-lives of proteins are often associated with more protein interactions (Li et al., 2021), it is expected that the glycan can stabilize proteins while regulating protein interactions with other biomolecules.

The $\log_2$ ratios were also calculated based on the half-lives of well-localized glycosylation sites compared with the corresponding non-modified proteins. The relationships between the effect of O-GlcNAcylation on protein dynamics among the nuclear glycoproteins with disorderedness and solvent accessibility were examined site specifically (Figure 6G). It was found that O-GlcNAcylation sites on ordered and buried regions play a more important role in enhancing the protein stability. Next, nuclear O-GlcNAcylation sites were clustered based on whether their positions were adjacant to (±10 amino acid residues) or within a domain, and their $\log_2$ ratios were compared (Figure 6H). The sites close to a domain show a significantly higher stabilizing effect than those far from any domain. These results demonstrate that the locations of the sites are critical for stabilizing glycoproteins.

O-GlcNAcylation was reported to be involved in the crosstalk with other modifications, such as ubiquitilation and phosphorylation, and the crosstalk may be relevant to the dynamics of proteins (Ruan et al., 2013). The nuclear O-GlcNAcylation sites were clustered based on whether they have nearby ubiquitination sites or have both ubiquitination and phosphorylation sites nearby (±10 amino acid residues). Compared with those without an adjacent ubiquitination site, O-GlcNAcylation sites with known ubiquitination sites nearby significantly further extended their half-lives. As phosphorylation can induce ubiquitination (Hunter, 2007), the O-GlcNAcylation sites adjacent to the both modifications were grouped, and their $\log_2$ ratios were also significantly higher than those with no ubiquitination sites nearby (Figure 6I). These results agree with the previous observation that O-GlcNAcylation had extensive crosstalk with phosphorylation and ubiquitination to regulate the protein degradation through the proteasome (Ruan et al., 2013).

PEST is a polypeptide sequence that is enriched with proline (P), glutamic acid (E), serine (S), and threonine (T). The sequence was reported to serve as a signal for fast proteolysis (Rechsteiner and Rogers, 1996). The average $\log_2$ ratio of those close to the PEST sequence is higher than those far away, suggesting that O-GlcNAcylation could protect proteins by modulating the function of the PEST sequence (Figure S5). Caspase is a cysteine protease that is activated in apoptosis (Li and Yuan, 2008). O-GlcNAcylation may also be involved in the proteolytic cleavage process by caspases. The caspase cleavage sites were predicted among the glycoproteins, and the nuclear O-GlcNAcylation sites were grouped based on whether they are adjacent to (±10 amino acid residues) any caspase cleavage sites. O-GlcNAcylation sites near the cleavage sites catalyzed by caspase 2 (CASP2), caspase 3 (CASP3), and caspase 7 (CASP7) have higher average $\log_2$ ratios (Figure 6J), suggesting that O-GlcNAcylation may prevent proteins from degradation by caspases. Overall, the current results demonstrate that O-GlcNAcylation can protect proteins through various mechanisms.

### Effect of OGA on the dynamics of O-GlcNAcylated proteins

The turnover of O-GlcNAcylated proteins can be due to either the enzymatic removal of O-GlcNAc by OGA or protein backbone degradation. To study the effect of OGA on the dynamics of O-GlcNAcylated proteins, we performed an experiment to quantify the degradation rates of O-GlcNAcylated proteins in the nucleus and the cytoplasm with the inhibition of OGA by Thiamet G (Yuzwa et al., 2008). In total, the half-lives of 228 and 232 O-GlcNAcylated proteins were quantified in the nucleus and the cytoplasm, respectively, with the treatment of Thiamet G (Figure S6A; Tables S7 and S8). With the Thiamet G treatment, the median half-lives of O-GlcNAcylated proteins in both the nucleus and the cytoplasm became longer (Figure 7A), with the half-lives of nuclear glycoproteins becoming >2 times longer (22.2 versus 47.4 h), and a relatively smaller increase for cytoplasmic glycoproteins (38.8 versus 49.1 h). The results indicate that OGA makes more contributions to the turnover of glycoproteins in the nucleus than those in the cytoplasm.

One critical function of O-GlcNAcylation is to regulate gene transcription. For the transcription factors quantified here, the half-lives of the O-GlcNAcylated and the non-modified forms, with or without the Thiamet G treatment, are included in Figures 7B and 7C. For most transcription factors quantitated here, their half-lives in the nucleus are much shorter than in the cytoplasm. With the treatment of the OGA inhibitor, the half-lives of many nuclear transcription factors were increased dramatically, but many of those in the cytoplasm underwent little or no change.

It is expected that the faster that OGA removes the glycan from glycoproteins, the larger the half-life changes upon the inhibitor treatment. To test this further, nuclear O-GlcNAcylation sites quantified under both the treated or untreated conditions were extracted, and the 21-mers with their adjacent sequences (±10

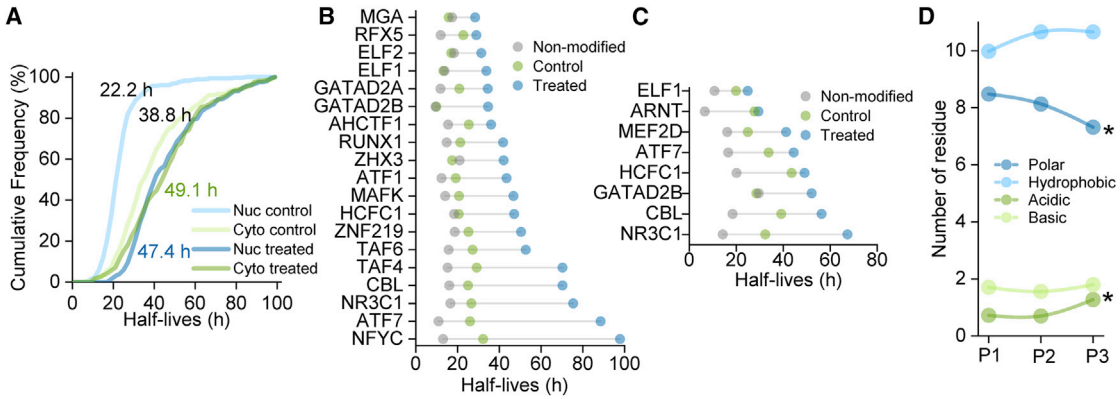


**Figure 7. Investigation of the effect of OGA on the dynamics of O-GlcNAcylated proteins**

(A) Distribution of the half-lives of O-GlcNAcylated proteins in the nucleus and the cytoplasm with or without the treatment of the OGA inhibitor.

(B and C) Comparison of the half-lives of O-GlcNAcylated transcription factors in the nucleus (B) and the cytoplasm (C) with or without the OGA inhibitor treatment.

(D) Evaluation of the effect of the adjacent residues on the half-life change for the nuclear O-GlcNAcylation sites. The acidic residues in P3 are significantly more than those in P1, while the polar residues are significantly less. The differences between the groups were calculated using the 2-sample t test, 2-tailed, and the significance levels are labeled *$p < 0.05$.

See also Figure S6 and Tables S7 and S8.

amino acids) were constructed. The sites were equally separated into three groups (P1, P2, and P3) based on the half-life changes with the OGA inhibition. Glycoproteins in P1 contained the sites with the smallest changes after the inhibitor treatment, while those in P3 had sites with the largest changes. The greater half-life changes were found to be correlated with more acidic and less polar residues near the glycosylation sites (Figure 7D). The sequence motif of the 21-mers from each group was generated to further evaluate the differences between the groups at certain positions (Figures S6B–S6D). P and V were overrepresented at −2 and −1, respectively, for all three groups. From +2 to +10, S and T were enriched for many residues in P1 and P2, but some of them were substituted by A and V in P3. The comparison results suggest that the half-lives of O-GlcNAcylation sites could be more dramatically extended by the OGA inhibition if hydrophobic amino acid residues instead of S or T were more enriched near glycosylation sites. The OGA substrate recognition was reported to be affected by the flanking residues around the glycosylation sites (Elbatrawy et al., 2020; Li et al., 2017). These results demonstrate further that the flanking residues around the glycosylation sites affect the glycan removal by OGA and the glycoprotein degradation rates.

## DISCUSSION

Recently, investigation of the spatial distributions of proteins at the proteome level has provided invaluable information to understand their interactions and functions (Lundberg and Borner, 2019). Protein PTMs play critical roles in their translocation, interactions, and dynamics. Previously, the distribution of modified proteins was constantly measured at the single-protein level (Wu et al., 2014). O-GlcNAcylation is the only known type of protein glycosylation in the nucleus and the cytoplasm, but the distributions of O-GlcNAcylated proteins in these two compartments have yet to be systematically investigated. Here, we systematically and site specifically studied the distributions of O-GlcNAcylated proteins in the nucleus and the cytoplasm. The integration of metabolic labeling and bioorthogonal chemistry allows for the selective enrichment of glycopeptides (Chen et al., 2015; Suttapitugsakul et al., 2020; Xiao et al., 2018). Benefitting from a cleavable linker, enriched glycopeptides were cleaved to generate a smaller mass tag for MS analysis. The distributions of many O-GlcNAcylated proteins were quantified using multiplexed proteomics. We found that O-GlcNAcylated proteins enriched in the nucleus or the cytoplasm have distinct functions. For instance, many nuclear-enriched glycoproteins are associated with nucleic acid binding, while many cytoplasmic-enriched glycoproteins are related to protein binding.

Site-specific analysis unravels the distributions of O-GlcNAcylated proteins with respect to the glycosylation sites. For example, GATAD2A with the O-GlcNAcylation site at T329 has a much higher nuclear distribution than the S625 or the S629 site, while no significant difference was found for the distribution of NUP214 with different sites. These results may be due to the fact that the O-GlcNAcylation can regulate protein translocation. Alternatively, the difference can be interpreted as some sites having regulatory roles and being preferentially modified in a certain compartment but others are not (Crook et al., 2020). This method advances our understanding of protein O-GlcNAcylation and can be used to study the distributions of proteins with other types of modifications.

Previously, the subcellular dynamics of the whole proteome and the phosphoproteome were quantified (Larance et al., 2013; Olsen et al., 2006), but studies focused on protein O-GlcNAcylation have not been reported. Here, the half-lives of O-GlcNAcylated proteins in the nucleus and the cytoplasm were quantified. The median half-life of O-GlcNAcylated proteins in the nucleus is 22.5 h, while that in the cytoplasm is approximately 2 times longer (38.8 h). The possible reason for the higher dynamics of nuclear glycoproteins

is that the glycan may be more actively removed in the nucleus, as supported by the results from the experiment with the treatment of the OGA inhibitor. The median half-life for glycoproteins in the nucleus increased >2 times with the OGA inhibition—much more than the half-life changes for glycoproteins in the cytoplasm. Another possibility for the longer-lived cytoplasmic glycoproteins could be related to the effect of co-translational O-GlcNAcylation preventing the ubiquitination of nascent polypeptides (Zhu et al., 2015), as protein translation occurs in the cytoplasm. Finally, we found the correlation between the distribution and the dynamics of O-GlcNAcylated proteins. Glycoprotein tends to have the higher cytoplasmic distribution when its half-lives in the nucleus and the cytoplasm are closer.

To demonstrate the effect of O-GlcNAcylation on protein turnover on a global scale, we simultaneously quantified the half-lives of the glycosylated and the non-modified forms of proteins. The results revealed that the majority of O-GlcNAcylated protein had longer half-lives than their non-modified counterparts in both the nucleus and the cytoplasm. Further analyses indicate that the O-GlcNAcylation sites located in the buried and ordered regions and next to a protein domain have stronger stabilizing effects against degradation. Previous studies showed that O-GlcNAcylation has the extensive crosstalk with phosphorylation and ubiquitination (Butkinaree et al., 2010). Accordingly, we also observed that O-GlcNAcylation sites adjacent to ubiquitination and phosphorylation sites further delayed protein degradation compared with those far from these sites. A similar effect was also found for O-GlcNAcylation sites close to the caspase cleavage sites. The present work further demonstrates the different mechanisms for the protective effect of O-GlcNAcylation on proteins.

### Limitations of the study

To enrich the low-abundance O-GlcNAcylated proteins, the cells were treated with Ac4GalNAz containing an azide group that enables the following selective enrichment. However, the azido group causes slight structural differences for the sugar analog from the original GlcNAc. Despite the slight difference, the azidosugar is a good mimic to study the distribution and dynamics of protein O-GlcNAcylation for the following reasons: First, the azido group is very small and biologically inert, and it has minimal cytotoxicity (Sletten and Bertozzi, 2009, 2011). Second, the incorporation of the azido group does not prevent O-GlcNAz to be added and removed by OGT and OGA, respectively, which are the only known enzymes for regulating the cycling of O-GlcNAcylation on protein substrates (Li et al., 2016; Zaro et al., 2011).

When an O-GlcNAcylated protein is very stable, the calculated half-life may not be very accurate, as the chase period is 24 h. Therefore, when the half-life was calculated to be >200 h, it was assigned as ''stable.'' In this case, it provides some information about the stability, but not the accurate half-life.

## STAR★METHODS

Detailed methods are provided in the online version of this paper and include the following:

- KEY RESOURCES TABLE
- RESOURCE AVAILABILITY
  - Lead contact
  - Materials availability
  - Data and code availability
- EXPERIMENTAL MODEL AND SUBJECT DETAILS
- METHODS DETAILS
  - Cell culture, metabolic labeling, and nucleus/cytoplasm isolation
  - Glycoprotein enrichment and digestion
  - TMT labeling and peptide fractionation
  - LC-MS/MS analysis
  - Database search and data filtering
  - Glycosylation site localization
  - Peptide and glycopeptide quantification
  - Bioinformatic analysis
- QUANTIFICATION AND STATISTICAL ANALYSIS

## SUPPLEMENTAL INFORMATION

Supplemental information can be found online at https://doi.org/10.1016/j.celrep.2022.110946.

## ACKNOWLEDGMENTS

We thank all of the group members in the Wu lab for inspiring discussions. This work was supported by grants to R.W. by the National Institute of General Medical Sciences of the National Institutes of Health (R01GM118803 and R01GM127711) and the National Science Foundation (CHE 2003597).

## AUTHOR CONTRIBUTIONS

R.W. conceived the study. S.X. and R.W. designed the experiments. S.X. performed the experiments. S.X., M.T., and S.S. analyzed the experimental data. R.W. raised the funds. S.X. and R.W. wrote the manuscript with input from all of the other authors.

## DECLARATION OF INTERESTS

The authors declare no competing interests.

Received: December 22, 2020
Revised: March 28, 2022
Accepted: May 23, 2022
Published: June 14, 2022

## REFERENCES

Agatemor, C., Buettner, M.J., Ariss, R., Muthiah, K., Saeui, C.T., and Yarema, K.J. (2019). Exploiting metabolic glycoengineering to advance healthcare. Nat. Rev. Chem. *3*, 605–620. https://doi.org/10.1038/s41570-019-0126-y.

Alfaro, J.F., Gong, C.X., Monroe, M.E., Aldrich, J.T., Clauss, T.R.W., Purvine, S.O., Wang, Z., Camp, D.G., 2nd, Shabanowitz, J., Stanley, P., et al. (2012). Tandem mass spectrometry identifies many mouse brain O-GlcNAcylated proteins including EGF domain-specific O-GlcNAc transferase targets. Proc. Natl. Acad. Sci. U. S. A. *109*, 7280–7285. https://doi.org/10.1073/pnas.1200425109.

Andrali, S.S., Qian, Q., and Ozcan, S. (2007). Glucose mediates the translocation of NeuroD1 by O-linked glycosylation. J. Biol. Chem. *282*, 15589–15596. https://doi.org/10.1074/jbc.m701762200.

Baldini, S.F., Wavelet, C., Hainault, I., Guinez, C., and Lefebvre, T. (2016). The nutrient-dependent O-GlcNAc modification controls the expression of liver fatty acid synthase. J. Mol. Biol. *428*, 3295–3304. https://doi.org/10.1016/j.jmb.2016.04.035.

Beausoleil, S.A., Villen, J., Gerber, S.A., Rush, J., and Gygi, S.P. (2006). A probability-based approach for high-throughput protein phosphorylation analysis and site localization. Nat. Biotechnol. *24*, 1285–1292. https://doi.org/10.1038/nbt1240.

Bernhofer, M., Goldberg, T., Wolf, S., Ahmed, M., Zaugg, J., Boden, M., and Rost, B. (2018). NLSdb-major update for database of nuclear localization signals and nuclear export signals. Nucleic Acids Res. *46*, D503–D508. https://doi.org/10.1093/nar/gkx1021.

Boyce, M., Carrico, I.S., Ganguli, A.S., Yu, S.H., Hangauer, M.J., Hubbard, S.C., Kohler, J.J., and Bertozzi, C.R. (2011). Metabolic cross-talk allows labeling of O-linked beta-N-acetylglucosamine-modified proteins via the N-acetylgalactosamine salvage pathway. Proc. Natl. Acad. Sci. U. S. A. *108*, 3141–3146. https://doi.org/10.1073/pnas.1010045108.

Butkinaree, C., Park, K., and Hart, G.W. (2010). O-linked beta-N-acetylglucosamine (O-GlcNAc): extensive crosstalk with phosphorylation to regulate signaling and transcription in response to nutrients and stress. Biochim. Biophys. Acta Gen. Subj. *1800*, 96–106. https://doi.org/10.1016/j.bbagen.2009.07.018.

Chen, W.X., Smeekens, J.M., and Wu, R.H. (2015). Systematic and site-specific analysis of N-sialoglycosylated proteins on the cell surface by integrating click chemistry and MS-based proteomics. Chem. Sci. *6*, 4681–4689. https://doi.org/10.1039/c5sc01124h.

Chen, Y., Liu, J., Zhang, W., Kadier, A., Wang, R., Zhang, H., and Yao, X. (2021). O-GlcNAcylation enhances NUSAP1 stability and promotes bladder cancer aggressiveness. OncoTargets Ther. *14*, 445–454. https://doi.org/10.2147/ott.s258175.

Cheng, S., Ren, J., Su, L., Liu, J., Liu, Q., Zhou, J., Ye, X., and Zhu, N. (2016). O-GlcNAcylation of the signaling scaffold protein, GNB2L1 promotes its degradation and increases metastasis of gastric tumours. Biochem. Biophys. Res. Commun. *478*, 1497–1502. https://doi.org/10.1016/j.bbrc.2016.08.074.

Crook, O.M., Smith, T., Elzek, M., and Lilley, K.S. (2020). Moving profiling spatial proteomics beyond discrete classification. Proteomics *20*, e1900392. https://doi.org/10.1002/pmic.201900392.

Cvitkovic, I., and Jurica, M.S. (2013). Spliceosome database: a tool for tracking components of the spliceosome. Nucleic Acids Res. *41*, D132–D141. https://doi.org/10.1093/nar/gks999.

de Queiroz, R.M., Madan, R., Chien, J., Dias, W.B., and Slawson, C. (2016). Changes in O-linked N-acetylglucosamine (O-GlcNAc) homeostasis activate the p53 pathway in ovarian cancer cells. J. Biol. Chem. *291*, 18897–18914. https://doi.org/10.1074/jbc.m116.734533.

Ding, X.D., Jiang, W., Zhou, P.P., Liu, L.L., Wan, X.L., Yuan, X.J., Wang, X.Z., Chen, M., Chen, J., Yang, J., et al. (2015). Mixed lineage leukemia 5 (MLL5) protein stability is cooperatively regulated by O-GlcNac transferase (OGT) and ubiquitin specific protease 7 (USP7). PLoS One *10*, e0145023. https://doi.org/10.1371/journal.pone.0145023.

Elbatrawy, A.A., Kim, E.J., and Nam, G. (2020). O-GlcNAcase: emerging mechanism, substrate recognition and small-molecule inhibitors. ChemMedChem *15*, 1244–1257. https://doi.org/10.1002/cmdc.202000077.

Elias, J.E., and Gygi, S.P. (2007). Target-decoy search strategy for increased confidence in large-scale protein identifications by mass spectrometry. Nat. Methods *4*, 207–214. https://doi.org/10.1038/nmeth1019.

Eng, J.K., McCormack, A.L., and Yates, J.R. (1994). An approach to correlate tandem mass-spectral data of peptides with amino-acid-sequences in a protein database. J. Am. Soc. Mass Spectrom. *5*, 976–989. https://doi.org/10.1016/1044-0305(94)80016-2.

Fu, X., Liang, C., Li, F., Wang, L., Wu, X., Lu, A., Xiao, G., and Zhang, G. (2018). The rules and functions of nucleocytoplasmic shuttling proteins. Int. J. Mol. Sci. *19*, 1445. https://doi.org/10.3390/ijms19051445.

Gama-Carvalho, M., and Carmo-Fonseca, M. (2001). The rules and roles of nucleocytoplasmic shuttling proteins. FEBS Lett. *498*, 157–163. https://doi.org/10.1016/s0014-5793(01)02487-5.

Han, J.W., Valdez, J.L., Ho, D.V., Lee, C.S., Kim, H.M., Wang, X.R., Huang, L., and Chan, J.Y. (2017). Nuclear factor-erythroid-2 related transcription factor-1 (Nrf1) is regulated by O-GlcNAc transferase. Free Radical Biol. Med. *110*, 196–205. https://doi.org/10.1016/j.freeradbiomed.2017.06.008.

Harreman, M.T., Kline, T.M., Milford, H.G., Harben, M.B., Hodel, A.E., and Corbett, A.H. (2004). Regulation of nuclear import by phosphorylation adjacent to nuclear localization signals. J. Biol. Chem. *279*, 20613–20621. https://doi.org/10.1074/jbc.m401720200.

Hart, G.W., Housley, M.P., and Slawson, C. (2007). Cycling of O-linked beta-N-acetylglucosamine on nucleocytoplasmic proteins. Nature *446*, 1017–1022. https://doi.org/10.1038/nature05815.

Hart, G.W., Slawson, C., Ramirez-Correa, G., and Lagerlof, O. (2011). Cross talk between O-GlcNAcylation and phosphorylation: roles in signaling, transcription, and chronic disease. Annu. Rev. Biochem. *80*, 825–858. https://doi.org/10.1146/annurev-biochem-060608-102511.

Hong, V., Presolski, S.I., Ma, C., and Finn, M.G. (2009). Analysis and optimization of copper-catalyzed azide-alkyne cycloaddition for bioconjugation. Angew. Chem. Int. Ed. *48*, 9879–9883. https://doi.org/10.1002/anie.200905087.

Hornbeck, P.V., Zhang, B., Murray, B., Kornhauser, J.M., Latham, V., and Skrzypek, E. (2015). PhosphoSitePlus, 2014: mutations, PTMs and recalibrations. Nucleic Acids Res. *43*, D512–D520. https://doi.org/10.1093/nar/gku1267.

Huang, D.W., Sherman, B.T., and Lempicki, R.A. (2009). Systematic and integrative analysis of large gene lists using DAVID bioinformatics resources. Nat. Protoc. *4*, 44–57. https://doi.org/10.1038/nprot.2008.211.

Hunter, S., Apweiler, R., Attwood, T.K., Bairoch, A., Bateman, A., Binns, D., Bork, P., Das, U., Daugherty, L., Duquenne, L., et al. (2009). InterPro: the integrative protein signature database. Nucleic Acids Res. *37*, D211–D215. https://doi.org/10.1093/nar/gkn785.

Hunter, T. (2007). The age of crosstalk: phosphorylation, ubiquitination, and beyond. Mol. Cell *28*, 730–738. https://doi.org/10.1016/j.molcel.2007.11.019.

Joiner, C.M., Li, H., Jiang, J., and Walker, S. (2019). Structural characterization of the O-GlcNAc cycling enzymes: insights into substrate recognition and catalytic mechanisms. Curr. Opin. Struct. Biol. *56*, 97–106. https://doi.org/10.1016/j.sbi.2018.12.003.

la Cour, T., Kiemer, L., Molgaard, A., Gupta, R., Skriver, K., and Brunak, S. (2004). Analysis and prediction of leucine-rich nuclear export signals. Protein Eng. Des. Sel. *17*, 527–536. https://doi.org/10.1093/protein/gzh062.

Lambert, S.A., Jolma, A., Campitelli, L.F., Das, P.K., Yin, Y., Albu, M., Chen, X., Taipale, J., Hughes, T.R., and Weirauch, M.T. (2018). The human transcription factors. Cell *172*, 650–665. https://doi.org/10.1016/j.cell.2018.01.029.

Lamond, A.I., and Earnshaw, W.C. (1998). Structure and function in the nucleus. Science *280*, 547–553. https://doi.org/10.1126/science.280.5363.547.

Lange, A., Mills, R.E., Lange, C.J., Stewart, M., Devine, S.E., and Corbett, A.H. (2007). Classical nuclear localization signals: definition, function, and interaction with importin $\alpha$. J. Biol. Chem. *282*, 5101–5105. https://doi.org/10.1074/jbc.r600026200.

Larance, M., Ahmad, Y., Kirkwood, K.J., Ly, T., and Lamond, A.I. (2013). Global subcellular characterization of protein degradation using quantitative proteomics. Mol. Cell. Proteomics *12*, 638–650. https://doi.org/10.1074/mcp.m112.024547.

Lefebvre, T., Ferreira, S., Dupont-Wallois, L., Bussiere, T., Dupire, M.J., Delacourte, A., Michalski, J.C., and Caillet-Boudin, M.L. (2003). Evidence of a balance between phosphorylation and O-GlcNAc glycosylation of Tau proteins - a role in nuclear localization. Biochim. Biophys. Acta Gen. Subj. *1619*, 167–176. https://doi.org/10.1016/s0304-4165(02)00477-4.

Levine, P.M., Balana, A.T., Sturchler, E., Koole, C., Noda, H., Zarzycka, B., Daley, E.J., Truong, T.T., Katritch, V., Gardella, T.J., et al. (2019). O-GlcNAc engineering of GPCR peptide-agonists improves their stability and in vivo activity. J. Am. Chem. Soc. *141*, 14210–14219. https://doi.org/10.1021/jacs.9b05365.

Levine, P.M., De Leon, C.A., Galesic, A., Balana, A., Marotta, N.P., Lewis, Y.E., and Pratt, M.R. (2017). O-GlcNAc modification inhibits the calpain-mediated cleavage of alpha-synuclein. Bioorg. Med. Chem. *25*, 4977–4982. https://doi.org/10.1016/j.bmc.2017.04.038.

Li, B., Li, H., Hu, C.W., and Jiang, J. (2017). Structural insights into the substrate binding adaptability and specificity of human O-GlcNAcase. Nat. Commun. *8*, 666. https://doi.org/10.1038/s41467-017-00865-1.

Li, F., Chen, J., Leier, A., Marquez-Lago, T., Liu, Q., Wang, Y., Revote, J., Smith, A.I., Akutsu, T., Webb, G.I., et al. (2020). DeepCleave: a deep learning predictor for caspase and matrix metalloprotease substrates and cleavage sites. Bioinformatics *36*, 1057–1065. https://doi.org/10.1093/bioinformatics/btz721.

Li, J., Cai, Z., Vaites, L.P., Shen, N., Mitchell, D.C., Huttlin, E.L., Paulo, J.A., Harry, B.L., and Gygi, S.P. (2021). Proteome-wide mapping of short-lived proteins in human cells. Mol. Cell *81*, 4722–4735.e5. https://doi.org/10.1016/j.molcel.2021.09.015.

Li, J., Wang, J., Wen, L., Zhu, H., Li, S., Huang, K., Jiang, K., Li, X., Ma, C., Qu, J., et al. (2016). An OGA-resistant probe allows specific visualization and accurate identification of O-GlcNAc-modified proteins in cells. ACS Chem. Biol. *11*, 3002–3006. https://doi.org/10.1021/acschembio.6b00678.

Li, J., and Yuan, J. (2008). Caspases in apoptosis and beyond. Oncogene *27*, 6194–6206. https://doi.org/10.1038/onc.2008.297.

Liu, C.F., Shi, Y.X., Li, J., Liu, X.W., Xiahou, Z., Zhikai, X.H., Tan, Z.P., Chen, X., and Li, J. (2020). O-GlcNAcylation of myosin phosphatase targeting subunit 1 (MYPT1) dictates timely disjunction of centrosomes. J. Biol. Chem. *295*, 7341–7349. https://doi.org/10.1074/jbc.ra119.012401.

Lo, P.W., Shie, J.J., Chen, C.H., Wu, C.Y., Hsu, T.L., and Wong, C.H. (2018). O-GlcNAcylation regulates the stability and enzymatic activity of the histone methyltransferase EZH2. Proc. Natl. Acad. Sci. U. S. A. *115*, 7302–7307. https://doi.org/10.1073/pnas.1801850115.

Luanpitpong, S., Rodboon, N., Samart, P., Vinayanuwattikun, C., Klamkhlai, S., Chanvorachote, P., Rojanasakul, Y., and Issaragrisil, S. (2020). A novel TRPM7/O-GlcNAc axis mediates tumour cell motility and metastasis by stabilising c-Myc and caveolin-1 in lung carcinoma. Br. J. Cancer *123*, 1289–1301. https://doi.org/10.1038/s41416-020-0991-7.

Lundberg, E., and Borner, G.H.H. (2019). Spatial proteomics: a powerful discovery tool for cell biology. Nat. Rev. Mol. Cell Biol. *20*, 285–302. https://doi.org/10.1038/s41580-018-0094-y.

Mahal, L.K., Yarema, K.J., and Bertozzi, C.R. (1997). Engineering chemical reactivity on cell surfaces through oligosaccharide biosynthesis. Science *276*, 1125–1128. https://doi.org/10.1126/science.276.5315.1125.

Marotta, N.P., Lin, Y.H., Lewis, Y.E., Ambroso, M.R., Zaro, B.W., Roth, M.T., Arnold, D.B., Langen, R., and Pratt, M.R. (2015). O-GlcNAc modification blocks the aggregation and toxicity of the protein alpha-synuclein associated with Parkinson's disease. Nat. Chem. *7*, 913–920. https://doi.org/10.1038/nchem.2361.

Martynova, N.Y., Parshina, E.A., and Zaraisky, A.G. (2021). Protocol for separation of the nuclear and the cytoplasmic fractions of Xenopus laevis embryonic cells for studying protein shuttling. STAR Protocols *2*, 100449. https://doi.org/10.1016/j.xpro.2021.100449.

Mckay, S.L., and Johnson, T.L. (2010). A bird's-eye view of post-translational modifications in the spliceosome and their roles in spliceosome dynamics. Mol. Biosyst. *6*, 2093–2102. https://doi.org/10.1039/c002828b.

Mitchell, A.L., Attwood, T.K., Babbitt, P.C., Blum, M., Bork, P., Bridge, A., Brown, S.D., Chang, H.Y., El-Gebali, S., Fraser, M.I., et al. (2019). InterPro in 2019: improving coverage, classification and access to protein sequence annotations. Nucleic Acids Res. *47*, D351–D360. https://doi.org/10.1093/nar/gky1100.

Mizuguchi-Hata, C., Ogawa, Y., Oka, M., and Yoneda, Y. (2013). Quantitative regulation of nuclear pore complex proteins by O-GlcNAcylation. Biochim. Biophys. Acta *1833*, 2682–2689. https://doi.org/10.1016/j.bbamcr.2013.06.008.

Nabbi, A., and Riabowol, K. (2015). Rapid isolation of nuclei from cells in vitro. Cold Spring Harb. Protoc. *2015*, pdb.prot083733. https://doi.org/10.1101/pdb.prot083733.

Ngoh, G.A., Watson, L.J., Facundo, H.T., and Jones, S.P. (2011). Augmented O-GlcNAc signaling attenuates oxidative stress and calcium overload in cardiomyocytes. Amino Acids *40*, 895–911. https://doi.org/10.1007/s00726-010-0728-7.

O'Shea, J.P., Chou, M.F., Quader, S.A., Ryan, J.K., Church, G.M., and Schwartz, D. (2013). pLogo: a probabilistic approach to visualizing sequence motifs. Nat. Methods *10*, 1211–1212. https://doi.org/10.1038/nmeth.2646.

Olsen, J.V., Blagoev, B., Gnad, F., Macek, B., Kumar, C., Mortensen, P., and Mann, M. (2006). Global, in vivo, and site-specific phosphorylation dynamics in signaling networks. Cell *127*, 635–648. https://doi.org/10.1016/j.cell.2006.09.026.

Pandurangan, A.P., Stahlhacke, J., Oates, M.E., Smithers, B., and Gough, J. (2019). The SUPERFAMILY 2.0 database: a significant proteome update and a new webserver. Nucleic Acids Res. *47*, D490–D494. https://doi.org/10.1093/nar/gky1130.

Petersen, B., Petersen, T.N., Andersen, P., Nielsen, M., and Lundegaard, C. (2009). A generic method for assignment of reliability scores applied to solvent accessibility predictions. BMC Struct. Biol. *9*, 51. https://doi.org/10.1186/1472-6807-9-51.

Poon, I.K.H., and Jans, D.A. (2005). Regulation of nuclear transport: central role in development and transformation? Traffic *6*, 173–186. https://doi.org/10.1111/j.1600-0854.2005.00268.x.

Qin, W., Lv, P., Fan, X., Quan, B., Zhu, Y., Qin, K., Chen, Y., Wang, C., and Chen, X. (2017). Quantitative time-resolved chemoproteomics reveals that stable O-GlcNAc regulates box C/D snoRNP biogenesis. Proc. Natl. Acad. Sci. U. S. A. *114*, E6749–E6758. https://doi.org/10.1073/pnas.1702688114.

Rechsteiner, M., and Rogers, S.W. (1996). PEST sequences and regulation by proteolysis. Trends Biochem. Sci. *21*, 267–271. https://doi.org/10.1016/s0968-0004(96)10031-1.

Ruan, H.B., Han, X.M., Li, M.D., Singh, J.P., Qian, K., Azarhoush, S., Zhao, L., Bennett, A.M., Samuel, V.T., Wu, J., et al. (2012). O-GlcNAc transferase/host cell factor C1 complex regulates gluconeogenesis by modulating PGC-1 alpha stability. Cell Metab. *16*, 226–237. https://doi.org/10.1016/j.cmet.2012.07.006.

Ruan, H.B., Nie, Y., and Yang, X. (2013). Regulation of protein degradation by O-GlcNAcylation: crosstalk with ubiquitination. Mol. Cell. Proteomics *12*, 3489–3497. https://doi.org/10.1074/mcp.r113.029751.

Ruba, A., and Yang, W.D. (2016). O-GlcNAc-ylation in the nuclear pore complex. Cell. Mol. Bioeng. *9*, 227–233. https://doi.org/10.1007/s12195-016-0440-0.

Sletten, E.M., and Bertozzi, C.R. (2009). Bioorthogonal chemistry: fishing for selectivity in a sea of functionality. Angew. Chem. Int. Ed. *48*, 6974–6998. https://doi.org/10.1002/anie.200900942.

Sletten, E.M., and Bertozzi, C.R. (2011). From mechanism to mouse: a tale of two bioorthogonal reactions. Acc. Chem. Res. *44*, 666–676. https://doi.org/10.1021/ar200148z.

Song, T.J., Zou, Q.L., Yan, Y.Y., Lv, S.L., Li, N., Zhao, X.F., Ma, X.Y., Liu, H.G., Tang, B.R., and Sun, L.D. (2021). DOT1L O-GlcNAcylation promotes its protein stability and MLL-fusion leukemia cell proliferation. Cell Rep. *36*, 109739. https://doi.org/10.1016/j.celrep.2021.109739.

Srikanth, B., Vaidya, M.M., and Kalraiya, R.D. (2010). O-GlcNAcylation determines the solubility, filament organization, and stability of keratins 8 and 18. J. Biol. Chem. *285*, 34062–34071. https://doi.org/10.1074/jbc.m109.098996.

Suttapitugsakul, S., Sun, F.X., and Wu, R.H. (2020). Recent advances in glycoproteomic analysis by mass spectrometry. Anal. Chem. *92*, 267–291. https://doi.org/10.1021/acs.analchem.9b04651.

Suttapitugsakul, S., Tong, M., Sun, F., and Wu, R. (2021a). Enhancing comprehensive analysis of secreted glycoproteins from cultured cells without serum starvation. Anal. Chem. *93*, 2694–2705. https://doi.org/10.1021/acs.analchem.0c05126.

Suttapitugsakul, S., Tong, M., and Wu, R.H. (2021b). Time-resolved and comprehensive analysis of surface glycoproteins reveals distinct responses of monocytes and macrophages to bacterial infection. Angew. Chem. Int. Ed. *133*, 11595–11604. https://doi.org/10.1002/ange.202102692.

Suttapitugsakul, S., Ulmer, L.D., Jiang, C.D., Sun, F.X., and Wu, R.H. (2019). Surface glycoproteomic analysis reveals that both unique and differential expression of surface glycoproteins determine the cell type. Anal. Chem. *91*, 6934–6942. https://doi.org/10.1021/acs.analchem.9b01447.

Suzuki, K., Bose, P., Leong-Quong, R.Y., Fujita, D.J., and Riabowol, K. (2010). REAP: a two minute cell fractionation method. BMC Res. Notes *3*, 294. https://doi.org/10.1186/1756-0500-3-294.

Tan, W., Jiang, P., Zhang, W., Hu, Z., Lin, S., Chen, L., Li, Y., Peng, C., Li, Z., Sun, A., et al. (2021). Posttranscriptional regulation of de novo lipogenesis by glucose-induced O-GlcNAcylation. Mol. Cell *81*, 1890–1904.e7. https://doi.org/10.1016/j.molcel.2021.02.009.

Tan, Z.W., Fei, G., Paulo, J.A., Bellaousov, S., Martin, S.E.S., Duveau, D.Y., Thomas, C.J., Gygi, S.P., Boutz, P.L., and Walker, S. (2020). O-GlcNAc regulates gene expression by controlling detained intron splicing. Nucleic Acids Res. *48*, 5656–5669. https://doi.org/10.1093/nar/gkaa263.

Tarbet, H.J., Toleman, C.A., and Boyce, M. (2018). A sweet embrace: control of protein-protein interactions by O-linked beta-N-acetylglucosamine. Biochemistry *57*, 13–21. https://doi.org/10.1021/acs.biochem.7b00871.

Torres, C.R., and Hart, G.W. (1984). Topography and polypeptide distribution of terminal N-acetylglucosamine residues on the surfaces of intact lymphocytes. Evidence for O-linked GlcNAc. J. Biol. Chem. *259*, 3308–3317. https://doi.org/10.1016/s0021-9258(17)43295-9.

UniProt, C. (2019). UniProt: a worldwide hub of protein knowledge. Nucleic Acids Res. *47*, D506–D515. https://doi.org/10.1093/nar/gky1049.

van der Laarse, S.A.M., Leney, A.C., and Heck, A.J.R. (2018). Crosstalk between phosphorylation and O-GlcNAcylation: friend or foe. FEBS J. *285*, 3152–3167. https://doi.org/10.1111/febs.14491.

Verspurten, J., Gevaert, K., Declercq, W., and Vandenabeele, P. (2009). SitePredicting the cleavage of proteinase substrates. Trends Biochem. Sci. *34*, 319–323. https://doi.org/10.1016/j.tibs.2009.04.001.

Vocadlo, D.J., Hang, H.C., Kim, E.J., Hanover, J.A., and Bertozzi, C.R. (2003). A chemical approach for identifying O-GlcNAc-modified proteins in cells. Proc. Natl. Acad. Sci. U. S. A. *100*, 9116–9121. https://doi.org/10.1073/pnas.1632821100.

Wang, M.C., Herrmann, C.J., Simonovic, M., Szklarczyk, D., and von Mering, C. (2015). Version 4.0 of PaxDb: protein abundance data, integrated across model organisms, tissues, and cell-lines. Proteomics *15*, 3163–3168. https://doi.org/10.1002/pmic.201400441.

Wang, X.S., Yuan, Z.F., Fan, J., Karch, K.R., Ball, L.E., Denu, J.M., and Garcia, B.A. (2016). A novel quantitative mass spectrometry platform for determining protein O-GlcNAcylation dynamics. Mol. Cell. Proteomics *15*, 2462–2475. https://doi.org/10.1074/mcp.o115.049627.

Woo, C.M., Iavarone, A.T., Spiciarich, D.R., Palaniappan, K.K., and Bertozzi, C.R. (2015). Isotope-targeted glycoproteomics (IsoTaG): a mass-independent platform for intact N- and O-glycopeptide discovery and analysis. Nat. Methods *12*, 561–567. https://doi.org/10.1038/nmeth.3366.

Wu, D.M., Zhang, P., Liu, R.Y., Sang, Y.X., Zhou, C., Xu, G.C., Yang, J.L., Tong, A.P., and Wang, C.T. (2014). Phosphorylation and changes in the distribution of nucleolin promote tumor metastasis via the PI3K/Akt pathway in colorectal carcinoma. FEBS Lett. *588*, 1921–1929. https://doi.org/10.1016/j.febslet.2014.03.047.

Xiao, H., Tang, G.X., and Wu, R. (2016). Site-specific quantification of surface N-glycoproteins in statin-treated liver cells. Anal. Chem. *88*, 3324–3332. https://doi.org/10.1021/acs.analchem.5b04871.

Xiao, H., and Wu, R. (2017). Quantitative investigation of human cell surface N-glycoprotein dynamics. Chem. Sci. *8*, 268–277. https://doi.org/10.1039/c6sc01814a.

Xiao, H.P., Suttapitugsakul, S., Sun, F.X., and Wu, R.H. (2018). Mass spectrometry-based chemical and enzymatic methods for global analysis of protein glycosylation. Acc. Chem. Res. *51*, 1796–1806. https://doi.org/10.1021/acs.accounts.8b00200.

Yang, W.H., Kim, J.E., Nam, H.W., Ju, J.W., Kim, H.S., Kim, Y.S., and Cho, J.W. (2006). Modification of p53 with O-linked N-acetylglucosamine regulates p53 activity and stability. Nat. Cell Biol. *8*, 1074–1083. https://doi.org/10.1038/ncb1470.

Yang, W.H., Park, S.Y., Nam, H.W., Kim, D.H., Kang, J.G., Kang, E.S., Kim, Y.S., Lee, H.C., Kim, K.S., and Cho, J.W. (2008). NF kappa B activation is associated with its O-GlcNAcylation state under hyperglycemic conditions. Proc. Natl. Acad. Sci. U. S. A. *105*, 17345–17350. https://doi.org/10.1073/pnas.0806198105.

Yuan, A.Y., Tang, X.Y., and Li, J. (2021). Centrosomes: Til O-GlcNAc do us apart. Front. Endocrinol. *11*. https://doi.org/10.3389/fendo.2020.621888.

Yuzwa, S.A., Macauley, M.S., Heinonen, J.E., Shan, X.Y., Dennis, R.J., He, Y.A., Whitworth, G.E., Stubbs, K.A., McEachern, E.J., Davies, G.J., et al. (2008). A potent mechanism-inspired O-GlcNAcase inhibitor that blocks phosphorylation of tau in vivo. Nat. Chem. Biol. *4*, 483–490. https://doi.org/10.1038/nchembio.96.

Zachara, N.E., O'Donnell, N., Cheung, W.D., Mercer, J.J., Marth, J.D., and Hart, G.W. (2004). Dynamic O-GlcNAc modification of nucleocytoplasmic proteins in response to stress. J. Biol. Chem. *279*, 30133–30142. https://doi.org/10.1074/jbc.m403773200.

Zaro, B.W., Yang, Y.Y., Hang, H.C., and Pratt, M.R. (2011). Chemical reporters for fluorescent detection and identification of O-GlcNAc-modified proteins reveal glycosylation of the ubiquitin ligase NEDD4-1. Proc. Natl. Acad. Sci. U. S. A. *108*, 8146–8151. https://doi.org/10.1073/pnas.1102458108.

Zecha, J., Satpathy, S., Kanashova, T., Avanessian, S.C., Kane, M.H., Clauser, K.R., Mertins, P., Carr, S.A., and Kuster, B. (2019). TMT labeling for the masses: a robust and cost-efficient, in-solution labeling approach. Mol. Cell. Proteomics *18*, 1468–1478. https://doi.org/10.1074/mcp.tir119.001385.

Zhang, F.X., Su, K.H., Yang, X.Y., Bowe, D.B., Paterson, A.J., and Kudlow, J.E. (2003). O-GlcNAc modification is an endogenous inhibitor of the proteasome. Cell *115*, 715–725. https://doi.org/10.1016/s0092-8674(03)00974-7.

Zhao, L., Feng, Z.H., Yang, X.Y., and Liu, J.K. (2016). The regulatory roles of O-GlcNAcylation in mitochondrial homeostasis and metabolic syndrome. Free Radic. Res. *50*, 1080–1088. https://doi.org/10.1080/10715762.2016.1239017.

Zhu, Y., Liu, T.-W., Madden, Z., Yuzwa, S.A., Murray, K., Cecioni, S., Zachara, N., and Vocadlo, D.J. (2016). Post-translational O-GlcNAcylation is essential for nuclear pore integrity and maintenance of the pore selectivity filter. J. Mol. Cell Biol. *8*, 2–16. https://doi.org/10.1093/jmcb/mjv033.

Zhu, Y., Liu, T.W., Cecioni, S., Eskandari, R., Zandberg, W.F., and Vocadlo, D.J. (2015). O-GlcNAc occurs cotranslationally to stabilize nascent polypeptide chains. Nat. Chem. Biol. *11*, 319–325. https://doi.org/10.1038/nchembio.1774.

## STAR★METHODS

### KEY RESOURCES TABLE

| REAGENT or RESOURCE | SOURCE | IDENTIFIER |
|---|---|---|
| Chemicals, peptides, and recombinant proteins | | |
| N-azidoacetylgalactosamine-tetraacetylated | Click Chemistry Tools | Cat#1086; CAS 653600-56-7 |
| N-acetylglucosamine-tetraacetylated | Synthose | Cat#AL363; CAS 3006-60-8 |
| Thiamet-G | Cayman chemical | Cat#13237; CAS 1009816-48-1 |
| cOmplete™, Mini, EDTA-free protease inhibitor cocktail | Sigma-Aldrich | Cat# 11836170001 |
| photocleavable (PC)-biotin-alkyne | Click Chemistry Tools | Cat#1118 |
| Tris(3-hydroxypropyltriazolylmethyl) amine | Click Chemistry Tools | Cat#1010; CAS 760952-88-3 |
| sodium L-ascorbate | Sigma-Aldrich | Cat#A7631; CAS 134-03-2 |
| aminoguanidine hydrochloride | Sigma-Aldrich | Cat#396494; CAS 1937-19-5 |
| sequencing grade modified trypsin | Promega | Cat#V5113 |
| Pierce™ high-capacity NeutrAvidin™ agarose | Thermo Fisher Scientific | Cat#29204 |
| TMTsixplex™ Isobaric Label Reagent Set | Thermo Fisher Scientific | Cat#90066 |
| hydroxylamine hydrochloride | Sigma-Aldrich | Cat#159417; CAS 5470-11-1 |
| Experimental models: Cell lines | | |
| Jurkat, Clone E6-1 | ATCC | Cat#TIB-152; RRID: CVCL_0367 |
| Software and algorithms | | |
| Xcalibur™ | Thermo Fisher Scientific | CAT#OPTON-30965 |
| SEQUEST | (Eng et al., 1994) | https://pubs.acs.org/doi/10.1021/jasms.8b00502 |
| Ascore | (Beausoleil et al., 2006) | https://www.nature.com/articles/nbt1240 |
| pLogo | (O'Shea et al., 2013) | https://plogo.uconn.edu/ |
| PAXdb | (Wang et al., 2015) | https://pax-db.org/ |
| SUPERFAMILY | (Pandurangan et al., 2019) | http://supfam.org/ |
| NetSurfP 1.1 | (Petersen et al., 2009) | http://www.cbs.dtu.dk/services/NetSurfP-1.1/ |
| NLSdb | (Bernhofer et al., 2018) | https://rostlab.org/services/nlsdb/ |
| NetNES 1.1 | (la Cour et al., 2004) | http://www.cbs.dtu.dk/services/NetNES/ |
| Spliceosome Database | (Cvitkovic and Jurica, 2013) | http://spliceosomedb.ucsc.edu/ |
| SitePrediction | (Verspurten et al., 2009) | https://www.dmbr.ugent.be/prx/bioit2-public/SitePrediction/index.php |
| Deposited data | | |
| Proteomics raw files | This study | MassIVE (MSV000089413) |
| proteomes - Homo sapiens (Human) | UniProt | https://www.uniprot.org/proteomes/UP000005640 |
| Database for Annotation, Visualization and Integrated Discovery (DAVID) | (Huang et al., 2009) | https://david.ncifcrf.gov/home.jsp |
| list of human transcription factors | (Lambert et al., 2018) | http://humantfs.ccbr.utoronto.ca/ |
| InterPro | (Hunter et al., 2009) | https://www.ebi.ac.uk/interpro/ |
| Others | | |
| UltiMate WPS-3000TPL RS Autosampler | Dionex | Cat#5826.0020 |
| UltiMate 3000 Rapid Separation Binary System | Thermo Fisher Scientific | Cat#IQLAAAGABHFAPBMBEZ |
| Orbitrap Elite™ Hybrid Ion Trap-Orbitrap Mass Spectrometer | Thermo Fisher Scientific | Cat#IQLAAEGAAPFADBMAZQ |

## RESOURCE AVAILABILITY

### Lead contact

Further information and requests for resources and reagents should be directed to and will be fulfilled by the lead contact, Ronghu Wu (ronghu.wu@chemistry.gatech.edu).

### Materials availability

This study did not generate new unique reagents.

### Data and code availability

- The raw files of proteomics data generated by MS are available in a publicly accessible website (MassIVE, massive.ucsd.edu) with the accession number of MSV000089413 (ftp://massive.ucsd.edu/MSV000089413/).
- This paper does not report original code.
- Any additional information required to reanalyze the data reported in this work paper is available from the lead contact upon request.

## EXPERIMENTAL MODEL AND SUBJECT DETAILS

Jurkat cells (from American Type Culture Collection, ATCC) were grown in RPMI-1640 medium (Sigma-Aldrich) containing 10% fetal bovine serum (FBS, Thermo) in a humidified incubator at 37°C with 5.0% $CO_2$. The cell density was monitored regularly.

## METHODS DETAILS

### Cell culture, metabolic labeling, and nucleus/cytoplasm isolation

When the density of Jurkat cells reached 2 × $10^6$ cells/mL, the medium was replaced with the one containing 100 μM N-azidoacetylgalactosamine-tetraacetylated ($Ac_4$GalNAz, Click Chemistry Tools) and the cells were further cultured for 48h. For the experiment to analyze the distribution of O-GlcNAcylated proteins, the cells were harvested directly by centrifugation. For the experiments to quantify the dynamics of O-GlcNAcylated proteins, the medium with light lysine (K0) and arginine (R0) was replaced with heavy lysine (K8) and heavy arginine (R6). $Ac_4$GalNAz was replaced with 100 μM N-acetylglucosamine-tetraacetylated ($Ac_4$GalNAc, Synthose). The cells were further cultured for 0, 3, 6, 9, 12, or 24 h, respectively, before being harvested. For the experiment with the OGA inhibitor treatment, Thiamet G (50 μM) was added to the media during the chase period to inhibit the removal of O-GlcNAc by OGA.

The harvested cells were washed with phosphate buffered saline (PBS) twice. Nucleus isolation was performed following previous publications (Nabbi and Riabowol, 2015; Wang et al., 2016). Briefly, the cells were resuspended into a nucleus isolation buffer containing 50 mM 4-(2-hydroxyethyl)-1-piperazineethanesulfonic acid (HEPES), pH = 7.4, 60 mM KCl, 50 μM Thiamet-G (Cayman chemical), 1 tablet/10 mL EDTA-free protease inhibitor (Roche), and 0.1% NP-40 (Sigma-Aldrich). The cell suspension was gently triturated for 5 times, incubated on ice for 3 min, and centrifuged at 500 g for 3 min. The pellets were separated from the supernatant and washed with the nucleus isolation buffer without NP-40. After centrifugation, the nuclear fraction was collected. For the cytoplasmic part, the supernatant was centrifuged at 500 g for 3 min and the precipitate, if any, was discarded. The supernatant was the cytoplasmic fraction. The cell nuclei were lysed in a buffer containing 50 mM HEPES, pH = 7.4, 150 mM NaCl, 0.5% SDC, 0.1% SDS, 1% NP-40, 50 μM Thiamet G, 50 units/mL Benzonase® nuclease (Millipore) and 1 tablet/10 mL EDTA-free protease inhibitor for 2 h at 4°C. After lysis, 5% of the cell lysate from each sample was separated for the whole proteome degradation analysis, and the rest were used for O-GlcNAcylated protein dynamics analysis.

### Glycoprotein enrichment and digestion

O-GlcNAcylated proteins labeled with the azido group in the lysates were tagged through the copper(I)-catalyzed azide-alkyne cycloaddition (CuAAC) reaction. Briefly, 250 μM photocleavable (PC)-biotin-alkyne (Click Chemistry Tools), 1 mM $CuSO_4$, 5 mM Tris(3-hydroxypropyltriazolylmethyl) amine (THPTA, Click Chemistry Tools), and 5% DMSO were added to the lysate. After thorough mixing, freshly prepared 15 mM sodium L-ascorbate (Sigma) and 15 mM aminoguanidine hydrochloride (Sigma) were added to initiate the reaction. The reaction was protected from light and lasted for 2 h at room temperature. Then, the reaction was quenched, and the proteins were purified using the methanol-chloroform precipitation method.

Proteins were digested with sequencing grade modified trypsin (Promega) with the ratio of protein: trypsin = 100: 1 in the digestion buffer (50 mM HEPES, pH = 8.6 and 1.6 M urea) at 37°C for 16 h. After protein digestion, the peptides were desalted using a tC18 Sep-Pak cartridge (Waters). Then the purified peptides were enriched with high-capacity NeutrAvidin™ agarose resins (Thermo) according to manufacturer's protocol. The peptides were incubated with the NeutrAvidin resins for 1 h at room temperature. The resins were then transferred to a spin column, washed 10 times with 100 mM PBS and 2 times with water. Finally, the resin was resuspended in water, and transferred to a glass vial, and the enriched glycopeptides were eluted under UV radiation at 350 nm for 1 h at room temperature. The eluent was frozen, lyophilized, and stored at −80°C for future use.

Proteins in the cell lysates for the whole proteome degradation were precipitated using the methanol-chloroform precipitation method, and then they were digested with trypsin for 16 h at 37°C. The digestion was quenched by adding trifluoroacetic acid (TFA) to a final concentration of 0.4%. The resulting peptides were desalted using the SepPak tC18 cartridges (Waters) and freeze-dried before TMT labeling.

### TMT labeling and peptide fractionation

For the analysis of O-GlcNAcylated protein distribution, three nuclear samples from the triplicate experiments were labeled with the first three channels (126, 127, and 128) of the TMT sixplex reagents (Thermo), and three samples of the cytoplasmic fractions were labeled with the other three channels (129, 130, and 131), respectively. The TMT labeling approach was adopted from the reported protocol with slight modification (Zecha et al., 2019). Briefly, the lyophilized peptides were resuspended in 33 μL of 100 mM HEPES, pH = 8.5 and 10 μL ACN. Each tube of the TMT labeling reagent was dissolved in 41 μL anhydrous ACN and then 10 μL of the solution was transferred to the designated sample. The labeling was performed for 1 h at room temperature, and the reaction was quenched by adding 4 μL of 10% hydroxyamine. The samples were mixed, lyophilized, and fractioned using the stage-tip method.

For the experiment to quantify the dynamics of O-GlcNAcylated proteins, the nuclear fractions and the cytoplasmic fractions at the six time points were separately labeled by one set of the TMT reagents. After the reaction, the six samples from the nuclear fraction were mixed as the nucleus sample (“Nuc”) and the cytoplasmic ones were mixed as the cytoplasm sample (“Cyto”). The glycopeptides were further purified using stage-tip and fractionated into six samples for LC-MS analysis. The TMT labeling for quantifying the dynamics of the non-modified proteins was the same as for the O-GlcNAcylated proteins. After labeling and mixing, the samples were fractionated into 40 fractions using high-pH reversed-phase high performance liquid chromatography (HPLC) with a 40-min gradient of 5-55% ACN in 10 mM ammonium formate (pH = 10). The fractions were combined into 20 samples and purified by stage-tip before LC-MS analysis.

### LC-MS/MS analysis

The peptides were resuspended in a solution containing 5% ACN and 4% FA, and 4 μL was loaded to a Dionex WPS-3000TPLRS autosampler (UltiMate 3000 thermostatted Rapid Separation Pulled Loop Wellplate Sampler) onto a microcapillary column packed with C18 beads (Magic C18AQ, 3 μm, 200 Å, 75 μm × 16 cm, Michrom Bioresources). The peptides were separated by reversed-phase HPLC using an UltiMate 3000 binary pump with a 120 min gradients of 2-32% ACN (with 0.125% FA). A hybrid dual-cell quadrupole linear ion trap - Orbitrap mass spectrometer (LTQ Orbitrap Elite, ThermoFisher, with Xcalibur 3.0.63 software) was coupled to HPLC for the identification and quantification of glycopeptides. The analysis was performed under a data-dependent Top15 method. For each cycle, a full MS scan with a resolution of 60,000 was followed by up to 15 tandem MS scans for the most intense ions at the resolution of 15,000. Both full and tandem MS were recorded in the Orbitrap cell with high resolution and high mass accuracy. The selected ions were excluded from further sequencing for 90 seconds. Ions with singly or unassigned charges were not selected for fragmentation. Higher-energy collision dissociation (HCD) with 34% normalized energy was employed to fragment the precursors.

### Database search and data filtering

The raw files were converted into mzXML files, and searched against the human (*Homo sapiens*) proteome database from UniProt using the SEQUEST algorithm (version 28) (Eng et al., 1994). The following parameters were used during the search: 20 ppm precursor mass tolerance; 0.025 Da product ion mass tolerance; up to two missed cleavages; up to three modifications on each peptide; fixed modifications: oxidation of methionine (+15.9949 Da), TMT modification of lysine and the peptide N-terminus (+229.1629 Da); variable modifications were used for glycopeptide search: glycosylation on serine, threonine, and cysteine (modified GlcNAc, +528.2859 Da). False discovery rates (FDR) of glycopeptide and glycoprotein identifications were evaluated by the target-decoy method (Elias and Gygi, 2007). Linear discriminant analysis (LDA) was employed to control the quality of glycopeptide identifications using multiple parameters, including XCorr, ΔCorr, missed cleavages, mass accuracy, peptide length and charge state. Peptides with fewer than seven amino acid residues were discarded. The FDRs of peptides were controlled to <1%, and the dataset was restricted to glycopeptides when determining FDRs for glycopeptides quantification.

### Glycosylation site localization

The confidence of glycosylation site localization was determined by ModScore, which is similar to Ascore. It employs a probabilistic algorithm that considers all possible glycosylation sites in a glycopeptide and uses the presence of experimental fragment ions unique to each site to find the best match (Beausoleil et al., 2006). Sites with ModScore > 13 ($p < 0.05$) were considered as confidently localized. In the earlier work published by our group, it was found that when cells were labeled with per-acetylated sugar analogs, protein S-glycosylation could occur, which may interfere with the identification of O-GlcNAcylation (Xiao and Wu, 2017). To remove S-glycosylation sites, we applied the following stringent criteria. First, during database search, serine, threonine, and cysteine were listed as possible glycosylation sites, and any glycopeptides with the modified GlcNAc localized on the cysteine residues were removed. Additionally, any identified O-GlcNAcylated peptides with a cysteine residue and the ModScore value of the site less than 13 (i.e., GlcNAcylation site not well-localized on S or T) were also removed. Eventually, only confidently identified glycopeptides with the glycan on the serine or threonine residue were kept.

### Peptide and glycopeptide quantification

For the quantification of the O-GlcNAc distribution, the ratios were calculated based on the intensities of the TMT reporter ions from the triplicate experiments (126/129, 127/130, and 128/131). The distribution ratio of each identified glycopeptide was the average value of the three ratios from the triplicate experiments. Furthermore, the protein distribution ratio was the average of three ratios from the triplicate experiments, which were calculated based on the median value of all peptide ratios from the same protein in each sample.

For the quantification of protein dynamics, the intensities of the reporter ions in the last five channels were used to calculate the ratios against the first one (126). For every unique glycopeptide, the ratio for each channel is the median of all ratios from the same peptides quantified here. For every glycoprotein, the ratio for each channel is the median of all ratios from all the peptides belonging to this protein. To calculate the half-lives of O-GlcNAcylated proteins, the six ratios were fitted using the exponential decay equation ($p = p_0 * e^{-kt}$). The half-life of any protein with $k < 0$, or with half-lives longer than 200 h were assigned as "stable" as their degradation rates cannot be accurately determined in the chase period of 24 h.

### Bioinformatic analysis

Protein functional annotation information was obtained from UniProt (UniProt, 2019) (https://www.uniprot.org/) and analyzed using the Database for Annotation, Visualization and Integrated Discovery (DAVID (Huang et al., 2009), https://david.ncifcrf.gov/). The list of human transcription factors was extracted from the Human Transcription Factors (Lambert et al., 2018) (http://humantfs.ccbr.utoronto.ca/). Only well-localized sites with the ModScore value of >13 were selected to perform the motif analysis using the online software (pLogo (O'Shea et al., 2013), https://plogo.uconn.edu/). Protein abundance information was found from the PAXdb database (Wang et al., 2015). Domain analysis was carried out using available information from the InterPro (Hunter et al., 2009) database, UniProt database, and the online prediction software SUPERFAMILY (Pandurangan et al., 2019). Protein secondary structures of the identified O-GlcNAcylated proteins were predicted by NetSurfP 1.1 (Petersen et al., 2009). Information of nuclear localization signal (NLS) was extracted from NLSdb (Bernhofer et al., 2018), and leucine-rich nuclear export signal (NES) was predicted by NetNES 1.1 (la Cour et al., 2004). The illustrations of chromatin, nuclear pore complex and spliceosome C complex were generated by BioRender (https://app.biorender.com/biorender-templates). Annotations of spliceosomal proteins were extracted from Spliceosome Database (Cvitkovic and Jurica, 2013). Transcription factors were annotated to different transcription factor families by InterPro (Mitchell et al., 2019). The information for protein physiochemical properties was extracted from the R package "Peptides" (https://github.com/dosorio/Peptides/). Ubiquitination and phosphorylation sites were extracted from the online website PhosphoSitePlus (https://www.phosphosite.org) (Hornbeck et al., 2015). The caspase cleavage sites were predicted by DeepCleave (Li et al., 2020). PEST sequences were predicted by SitePrediction (Verspurten et al., 2009).

## QUANTIFICATION AND STATISTICAL ANALYSIS

Statistical analysis was performed using Excel and OriginLab. The statistical details of the experiments can be found in the Results section and in figure legends. Significance was defined when p value was <0.05, and p values were calculated using the two-tailed Student's t test, two-tailed, unless otherwise stated.